9. TST SOFTWARE

9.1 NKRemote

NKRemote by Breeze Systems ($175) (http://www.breezesys.com/index.htm) facilitates remote control of Nikon digital SLR cameras from a microcomputer. It is ideally suited for the TST as several of the program's features are utilized including:

a) Live view on a computer monitor of the scene in the camera's field of view.

b) Full control of all camera settings from the computer.

c) Digital zooming on a zone of interest in the field of view.

d) Remote manual focusing on a zone of interest or on the full image.

e) Remote image capture and direct file storage to a computer hard drive.

9.2 ImageJ

ImageJ is a public domain image processing and analysis program developed at the U.S. National Institutes of Health (http://rsbweb.nih.gov/ij/index.html). It runs under Java. The major program features utilized for the TST test are:

a) Cropping images that were taken by NKRemote.

b) Adjusting threshold levels for conversion to binary images.

c) Converting images to binary (black and white) images.

d) Separating touching particles using *watershed segmentation*.

e) Counting segmented objects

f) Sizing segmented objects

9.3 TST.exe

TST.exe is an executable program that was developed at the University of Michigan using MATLAB by Mathworks. MATLAB is a high-level computer language that performs many mathematical tasks, particularly those involving matrix algebra, faster than traditional programming languages such as Fortran and C++. The TST program uses the number of pixels for each particle counted by ImageJ. It converts the particle pixel area distribution to a particle size distribution and outputs the test results with minimal user interaction. Since TST.exe is a compiled executable program, the user does not use MATLAB directly and will not need to have it installed on the TST system's microcomputer.

10. TST SYSTEM SET-UP

10.1 Camera System Installation

1) The height clearance between the surface of the camera lens and the surface of the translucent plate must be 7.6 ft. With this distance, the combination of the D7000 camera sensor (23.6 mm x 15.6 mm) and the 60 mm focal length of the camera lens, the field of view becomes the required 3 ft. x 2 ft. (i.e. the bottom two-thirds of the TST translucent plate). The variable screw positions on the camera bracket allow for this clearance to be achieved over a limited range of ceiling heights. For considerably taller ceilings, either the bracket system must be extended or the TST can be placed on an appropriately raised platform.

2) Install the ceiling bracket (with attached camera bracket) in the ceiling by laying its long dimension (24 in.) into the rails parallel to the short (24 in.) dimension of a drop ceiling panel. Of course, the ceiling panel must be removed or slotted to accommodate the 24 in. long x 3 in. wide ceiling bracket. The ceiling bracket should ideally be located at the end of a ceiling panel to take advantage of rail support on three sides (see photos of installed brackets in Chapter 8).

3) Attach the camera bracket using a mounting screw. The height of the camera can be adjusted up to +/- 2.2 in. by choosing various mounting holes.

4) Insert the EP-5 Nikon adaptor into the battery compartment of the camera and connect the EH-5A Nikon AC power cord with the adaptor. The direct power from a lab outlet eliminates the need for battery removal for charging.

5) Link the camera to the computer using the UC-E4 Nikon camera-to-computer cable. The USB socket can be found under the rubber panel of the D7000.

6) Level the camera using the bi-directional bubble level so that the surface of the camera lens is horizontal. The camera can be rotated in one direction using the mounting screw as a pivot. However, the ceiling bracket would have to be shimmed to level the camera in the orthogonal direction.

10.2 TST System Positioning

1) Level the translucent segregation table so that the surface of the translucent plate is horizontal.

2) Set the camera exposure mode to “manual” on the camera by turning the mode dial to < M >. Next, set the camera to autofocus by setting the mode switch on the lens to <M/A> and also setting the mode switch to < AF > on the camera.

3) Open <NKRemote> and adjust camera settings from the window that automatically appears to the following (these settings are appropriate for the backlit TST in a dark room):

Shutter speed (Tv) < 1/50 >
Aperture size (Av) < 10 >
Sensitivity (ISO) < 100 >
Exposure compensation < none >
Image quality < JPEG Normal >
Image size < Large 4928x3264 >
White balance < Auto >
Metering mode < Matrix >
Picture control < Standard >
Autofocus mode < Single >

Check the center focus point box from among the 39 focus point boxes.

4) Open live view by selecting < Camera > - < Live View > from the menu bar.
A full frame live view will appear.

5) The table will appear on the live view window. Position the table below the camera such that the bottom 3 ft. x 2 ft. appears in the field of view and is lined up with the edges of the photo.

10.3 Selection and Installation of Bridges

1) As many (or as few) of the 18 paired slots in the slotted side walls can be used for the segregation bridge. However, only the bottom 3 ft. x 2 ft. of the plate will be in the camera’s view. As such, all of the particles must eventually must end up in this zone. The number and location of the segregation bridges can be determined from pilot tests. Nevertheless, the following sequence of six underpass heights is common and corresponds to a typical sieve order:

19.1 mm, 12.7 mm, 9.5 mm, 4.8 mm, 3.2 mm, 2.2 mm.

Each underpass in this sequence is 70% +/- 5% of the previous underpass height thereby insuring that no particles should be able to hide behind others in their segregated group.

If the soil particles accumulate in large quantities between certain bridges, these bridges should be moved apart. It is again emphasized that the overall objective is to somewhat segregate the particles by size but only so far as to not allow small particles to hide beneath larger ones. Thus, the segregation need not be thorough and complete.

10.4 Establishing Image Scale

1) Turn off the TST backlight if it is on. Room lighting should be on.

2) Place a scale near the center of the translucent plate parallel to one of the plate edges. Adjust its orientation with the assistance of the NKRemote live view.

3) Zoom in on the scale by double clicking the green box in the live view screen. Also set the "Zoom" to 100% in the menu at the bottom of the window. By zooming in, a better focus can be achieved. Adjust the focus using small focus steps (single arrow at the bottom of the window). Note that this is digital zooming and not an actual zooming by the camera lens (it is not a zoom lens).

4) Change the aperture size (Av) of the camera from < 10 > to < 3.2 > for determining image scale. Take a photograph by clicking < Release > located on the bottom of the live view screen. Return (Av) to <10>. The temporary aperture change is needed only to have the ruler well-illuminated for image capture.

5) The captured image is automatically stored in c:\NKRemote\today's year-month-date.

4) Open the image using < Paint >. Using the magnifier tool (magnifying glass) at 6x setting, enlarge a 1 in. segment of the ruler. Next, choose the Select tool (dashed rectangle). Left-click and drag the long length of the rectangle to a width corresponding to 1 in. on the ruler. Keep the left mouse button pressed and note the width in pixels displayed on the bottom right corner of the screen. The value should be about 140 pixels; record it. Convert the resolution to pixels/mm by dividing the pixles/in. by 25.4. Round this value to 0.1 pixels/mm.

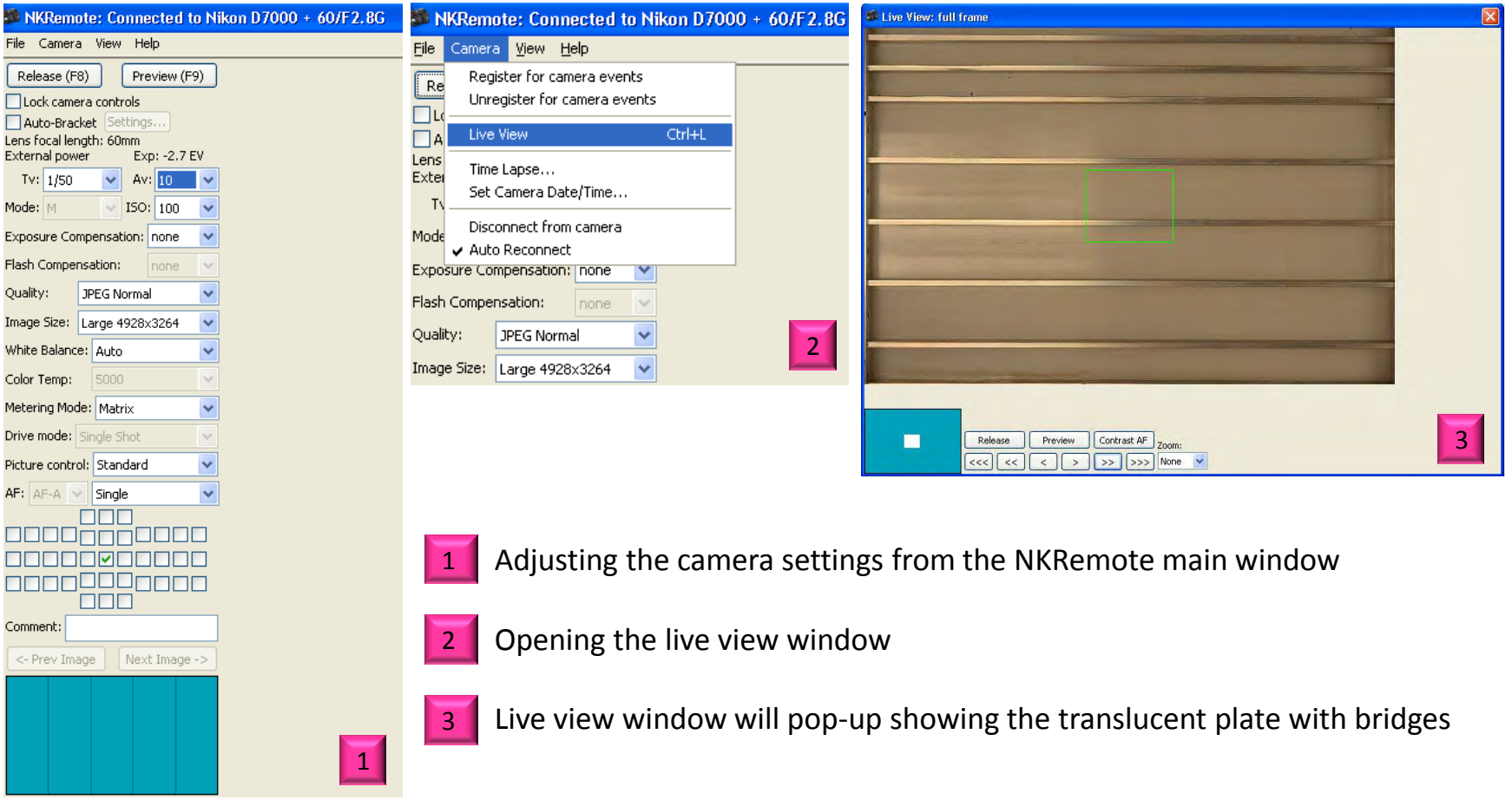

1 Adjusting the camera settings from the NKRemote main window

2 Opening the live view window

3 Live view window will pop-up showing the translucent plate with bridges

Fig. 10.1 Adjusting the camera settings and opening the live view window from NKRemote.

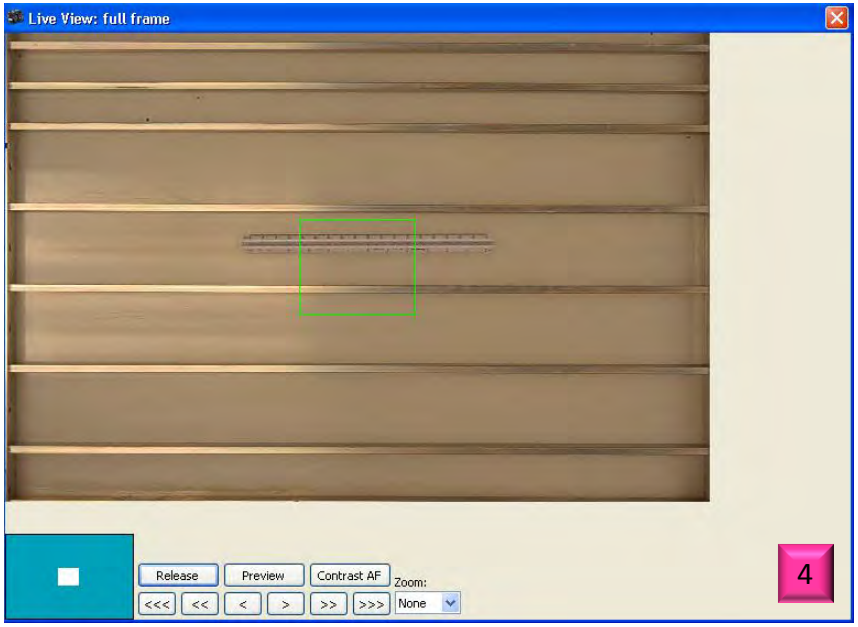

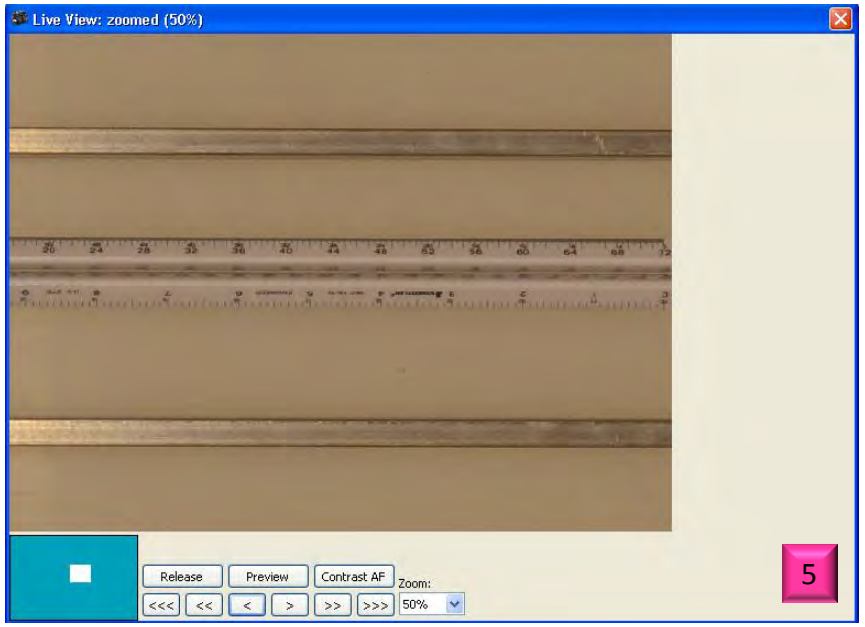

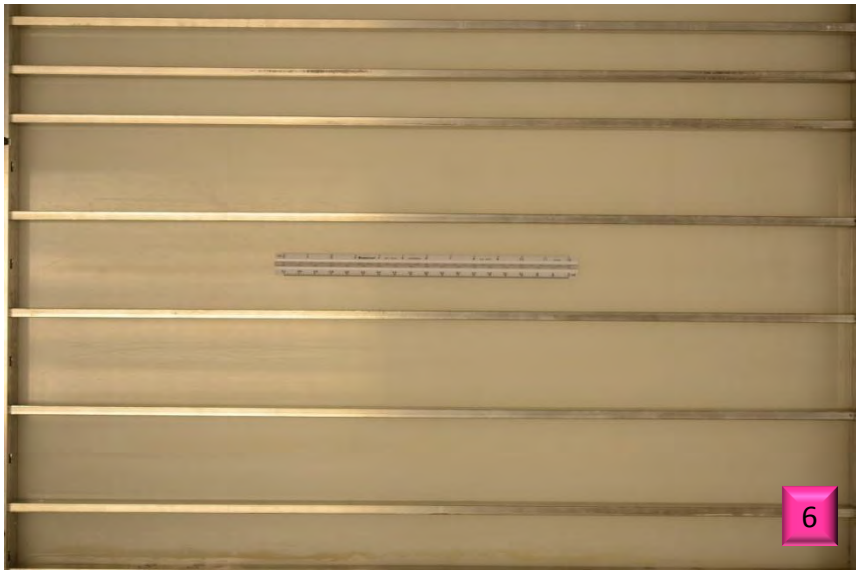

4 Placing a scale on the translucent plate

5 Fine-tuning the focus using the single arrow keys in the expanded view

6 Capturing an image

Fig. 10.2 Establishing image scale using a scale placed on the translucent plate.

11. TST TEST PROCEDURE

Sections 11.1 through 11.7 below have correspondingly numbered figures with 3 steps shown in each figure. Section 11.8 refers to the computer analysis and is therefore lengthier with 5 figures.

11.1 Introducing Specimen and Table Raising

1) Spread out dry soil particles on the translucent plate above the topmost bridge.
2) Lift the plate slowly using the two handles.
3) Allow the particles to slide or roll down the plate until they come to rest behind the bridges.

11.2 Immobilizing the Inclined Table

4) If not already released, remove the immobilizing screws to release the feet from their transport position.
5) Lower the two support feet to vertical positions.
6) Slip the two immobilizing screws through the holes in the feet and screw them into the threaded sockets near the base of the light table.

11.3 Brushing

7) Brush beneath the segregation bridges so that the blockages break down.
8) Occasionally also brush above the bridges.
9) Continue to brush for a minute or two until particles have stopped slipping beneath the bridges then lower the table to the horizontal position.

11.4 Tap-down

10) Distribute the particles over the area between the segregation bridges using the small brush. A vertical taping motion is most efficient.
11) Tap the corner of the table using the rubber mallet so that the remaining particle mounds collapse.

11.5 Removing the Bridges

12) Open the cover bars by releasing tightening screws.
13) Swing the cover bars outward to expose the bridge ends.
14) Remove the segregation bridges.

11.6 Image Capture

15) Make sure that all of the particles are in the camera's field of view. Using NKRemote focus on the segregated soil.
16) Turn on the light table and turn off the room lights.
17) Take a photograph.

11.7 Specimen Removal and Cleaning

18) Release the connector screw and remove the top wall.

19) Using the squeegee sweep out particles through the opening.
20) If necessary, wipe the translucent plate using a dust cloth.

11.8 Computer Analysis and Printout

21) Place the image of the segregated soil in the folder containing <TST.exe >.
22) Open < ImageJ >. The Commands menu will appear.
23) Select *File-Open*. Open the image of the segregated soil by selecting the image file.
24) Select *Process-Binary-Make Binary*. The image will become black & white.
25) Select *Process-Binary-Watershed*. This will separate the contacting particles.
26) Select *Analyze-Analyze Particles*. The *Analyze Particles* window will appear.
27) Check *Display Results* and *Clear Results*. The pixel area of each particle will be displayed in the *Results* window.
28) Select *File-Save As* from the *Results* window. Save the result in a text format in the same folder containing program <TST.exe>. Also save the image of the segregated soil in this folder.
29) Open < TST.exe > by right-clicking and selecting *Open* or double-clicking the file.
30) Input the requested soil and image information in two windows.
31) The TST test results will appear. They include:
    a) Specimen, test and image details;
    b) The captured image;
    c) Grain size distributions assuming (for comparison) both the equivalent diameter method and the minor ellipse axis method;
    d) A histogram of the particle aspect ratios versus grain size.
32) A table of test data is also produced. It includes the Fraction % Retained, Cumulative % Retained and the Results % Passing

The results may be printed and/or saved.

Finally, some tests will require significantly more than 1000 g of specimen for testing. The testing TST can be performed in stages using any number of 1000 g (or less) specimens and the results may be combined to produce a single size distribution. The tests presented in Appendix G were performed this way.

1 Soil particles are spread out on the translucent plate above the topmost bridge.

2 Plate is slowly lifted by the handles allowing the particles to roll and slide down incline passing beneath progressively smaller bridge underpasses.

3 Particles come to rest behind the bridges.

Fig. 11.1 Introducing specimen & table raising.

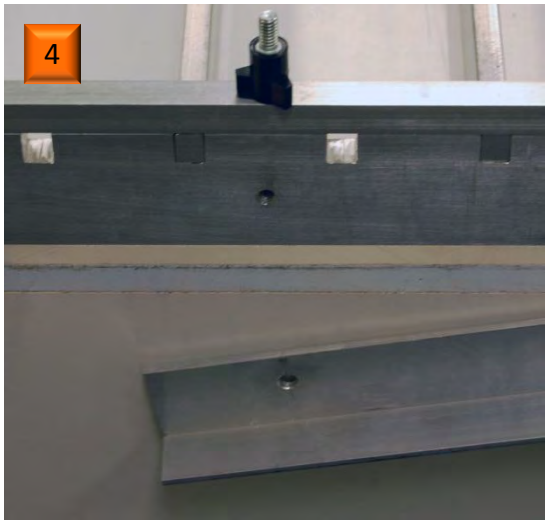

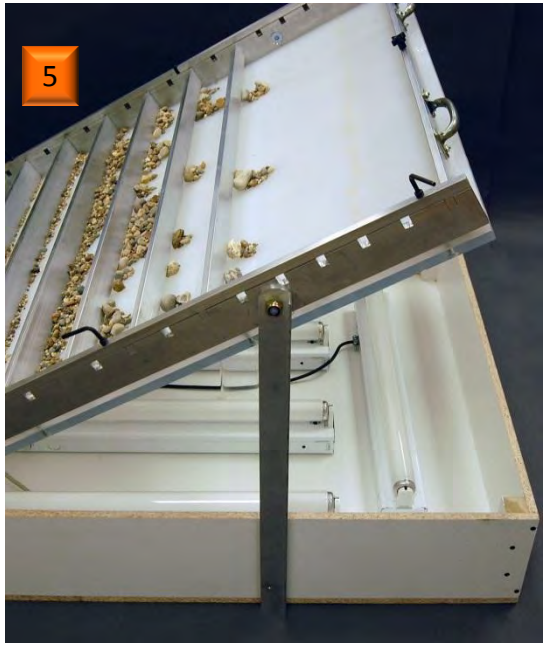

4 The two support feet are released

5 Feet are lowered to a vertical position

6 Immobilizing screw keeps feet from accidentally slipping out.

Fig. 11.2 Immobilizing the inclined table.

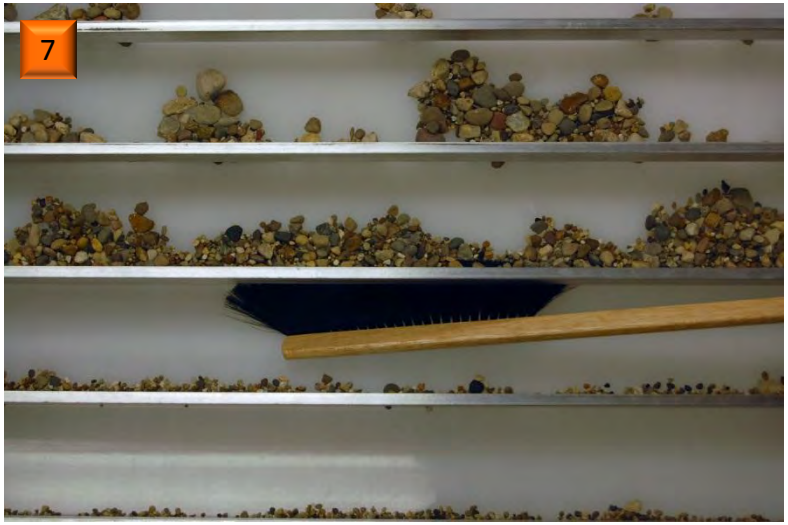

7 & 8 Brushing beneath (or above) bridges breaks down blockages.

9 Segregated particles ready for plate lowering.

Fig. 11.3 Brushing.

10 After plate lowering, gentle tapping with the small brush distributes the particles over the area between the bridges.

11 One or two light vertical taps with the rubber mallet over the corner of the table collapses the remaining particle mounds.

Fig. 11.4 Tapping-down.

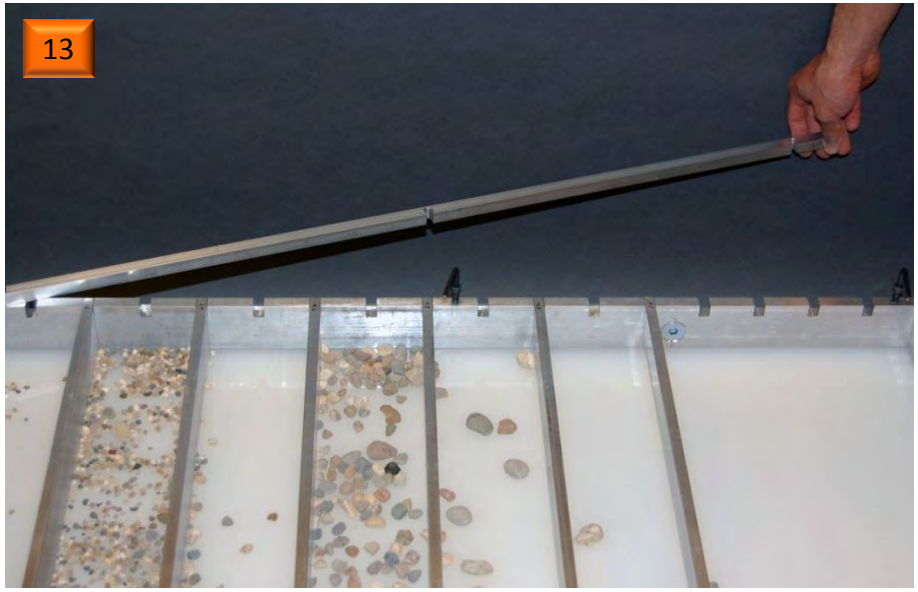

12 Quarter turn on tightening screws to release the cover bars

13 Cover bars swing outward from the slotted side walls

14 Bridges are removed

Fig. 11.5 Removing the bridges.

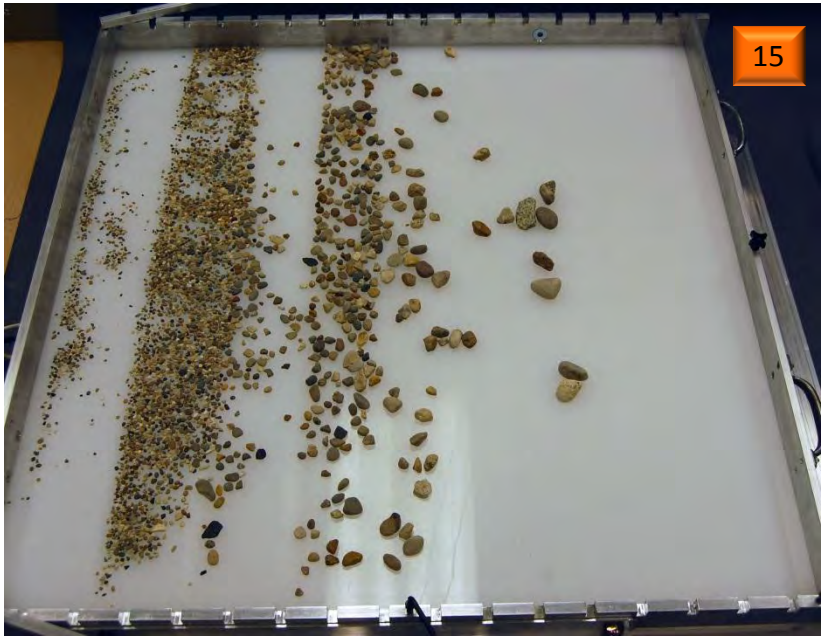

15 Quasi-segregated and shaken-down particles prepared for image capture.

16 Table lights are turned on.

17 Image captured by overhead camera remotely from computer.

Fig. 11.6 Image capture.

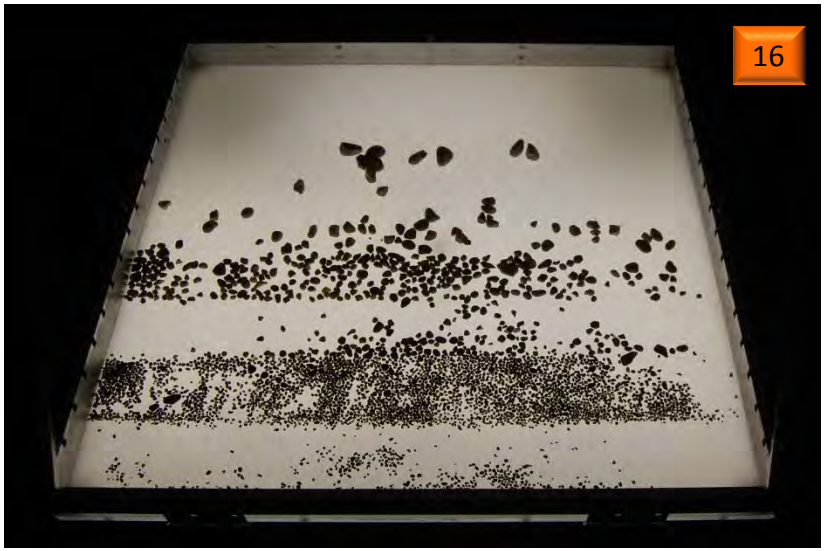

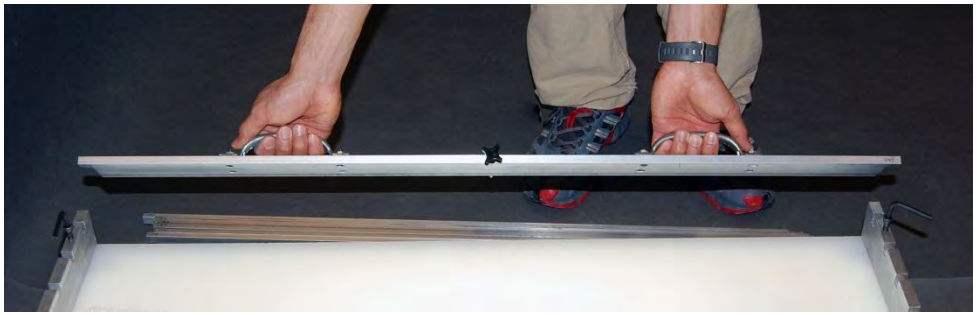

18 Connector screw removed and top plate lifted out.

19 Particles swept out through opening by a squeegee

20 Occasional dusting of plate surface

Fig. 11.7 Specimen removal & cleaning.

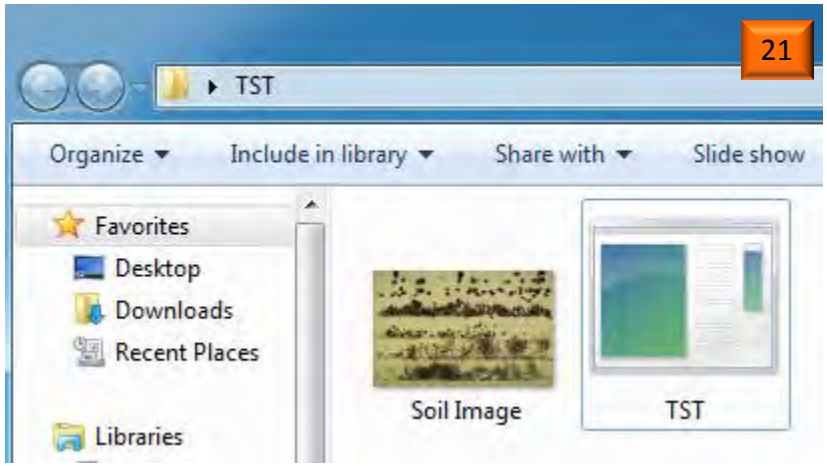

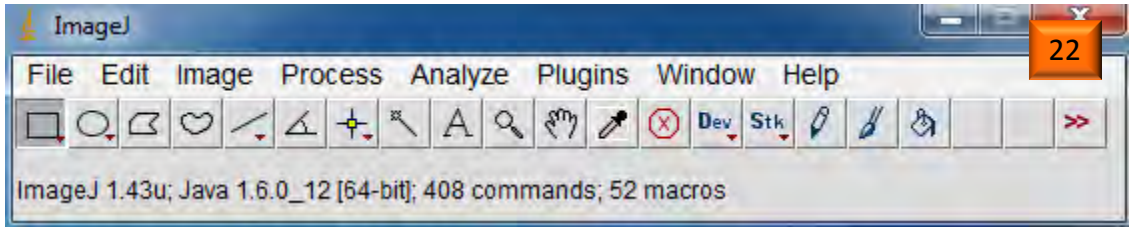

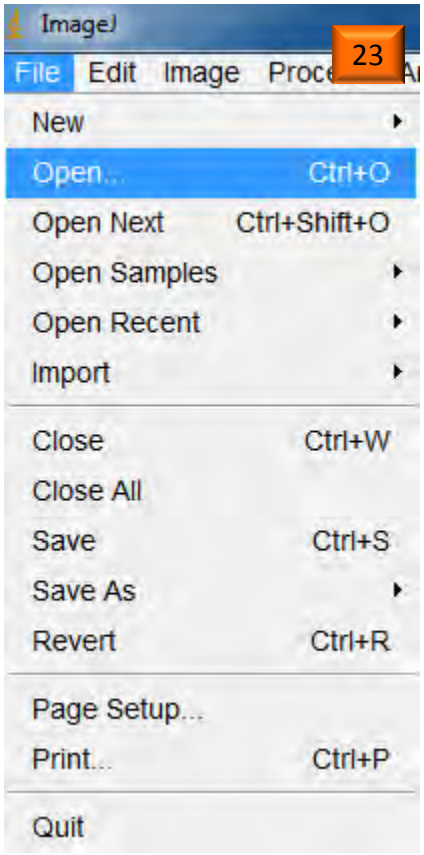

21 Placing the image of the segregated soil in the folder containing < TST.exe >.

22 Opening < ImageJ >. The Commands menu will appear.

23 Selecting *File-Open* and opening the image of the segregated soil by choosing the image file.

Fig. 11.8 Opening the image of the segregated soil in < ImageJ >.

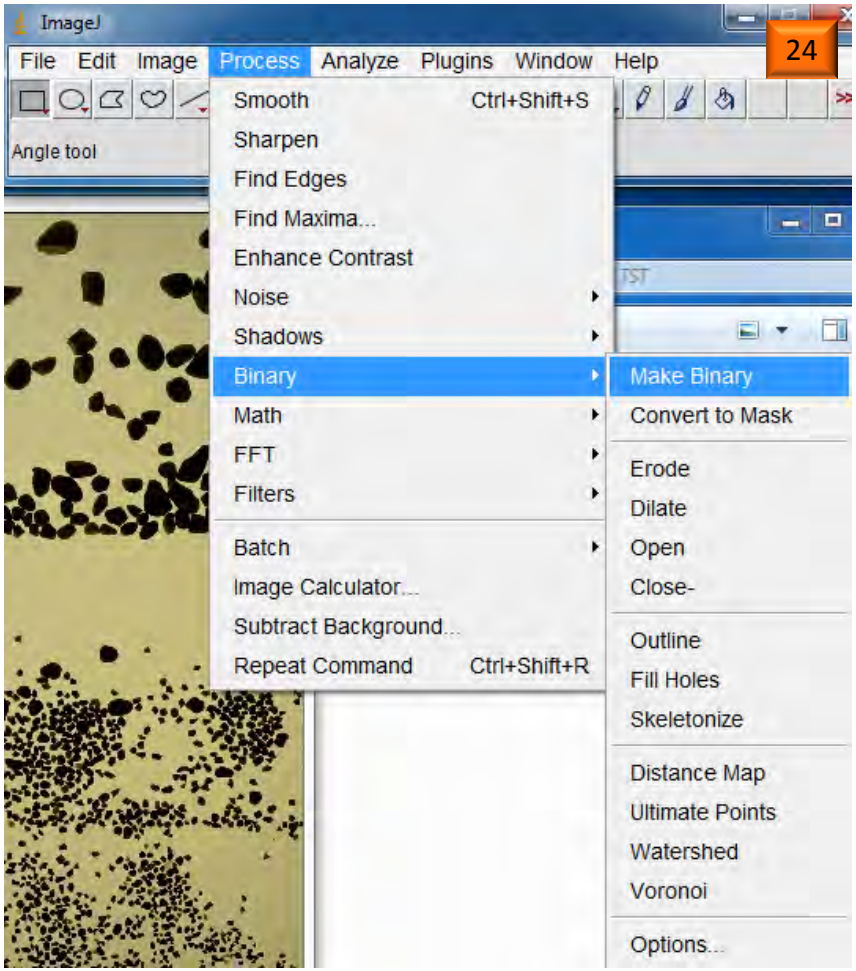

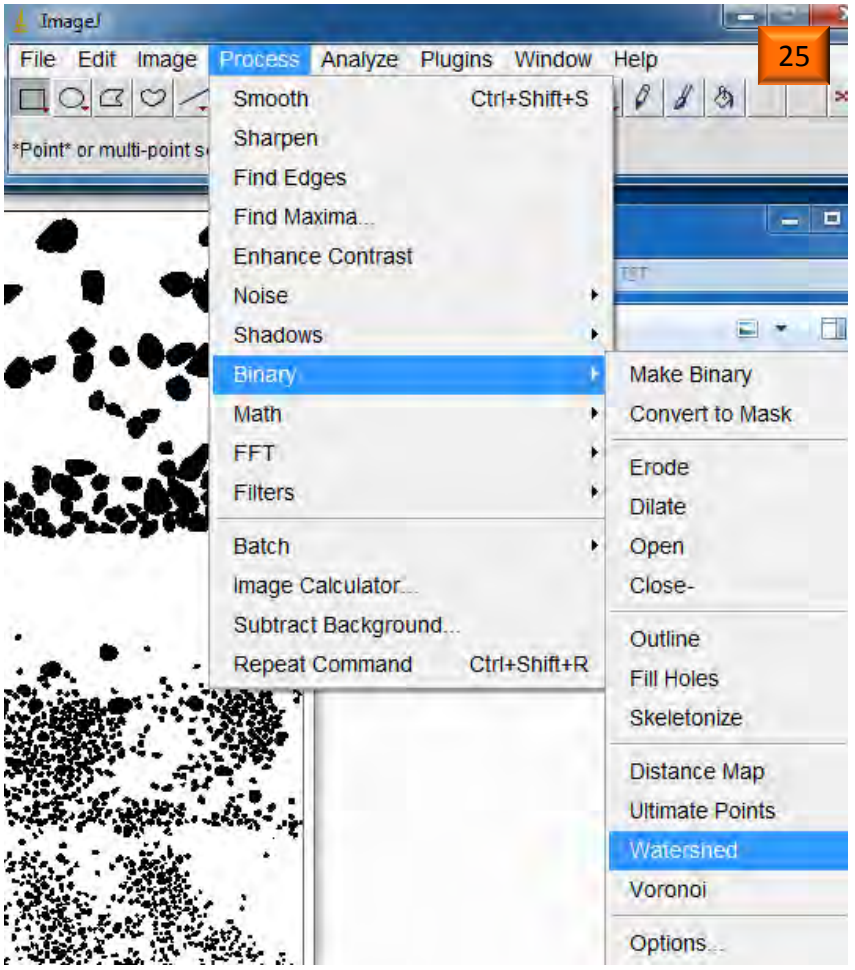

24 Selecting *Process-Binary-Make Binary.* The image will become black & white.

25 Selecting *Process-Binary-Watershed*. The particles will be separated.

Fig. 11.9 Converting to a binary image and separating particles by watershed segmentation.

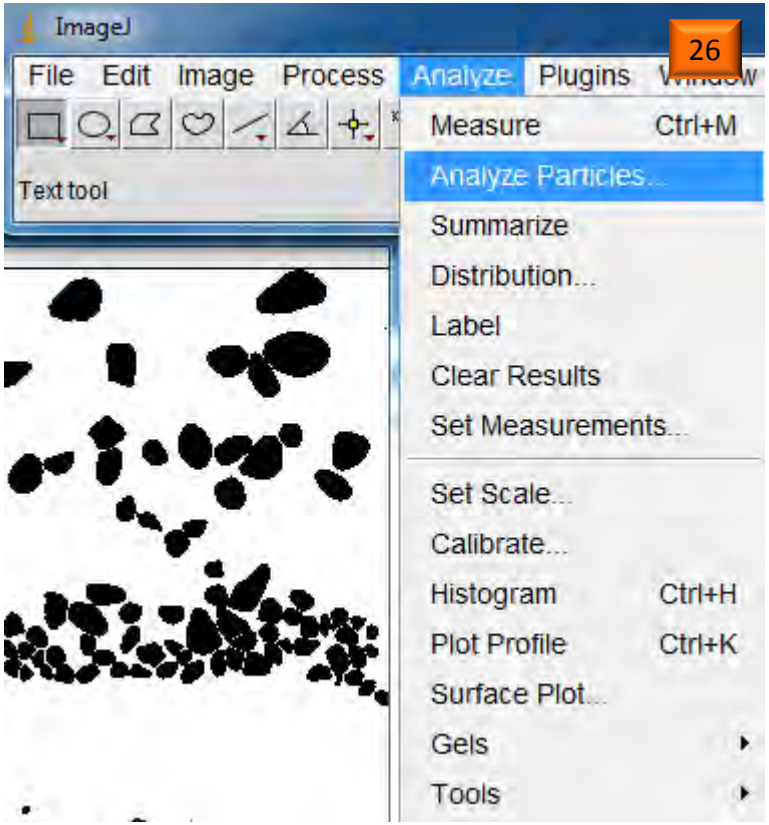

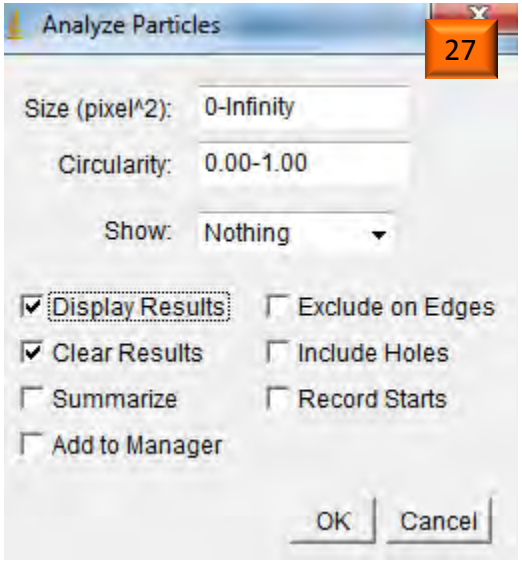

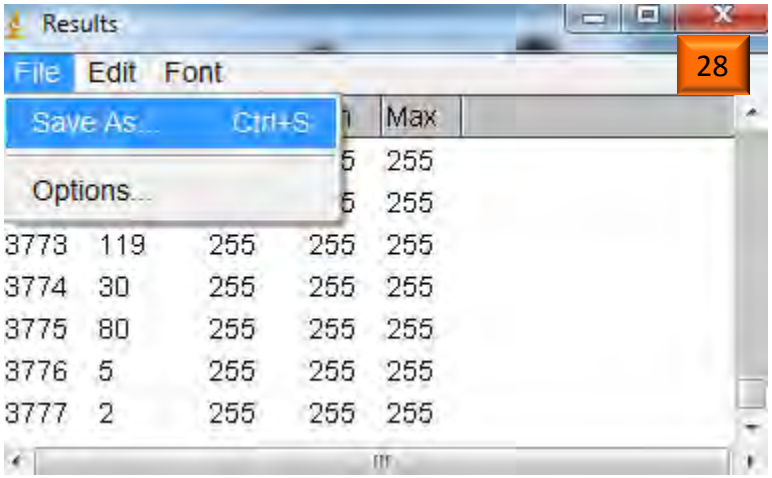

26 Selecting *Analyze-Analyze Particles*.

27 Checking *Display Results* and *Clear Results* in the *Analyze Particles* window.

28 Selecting *File-Save As* in the *Results* window. Saving the soil image and the results in a text format in the folder containing < TST.exe >.

Fig. 11.10 Saving the pixel areas of each particle in a text format.

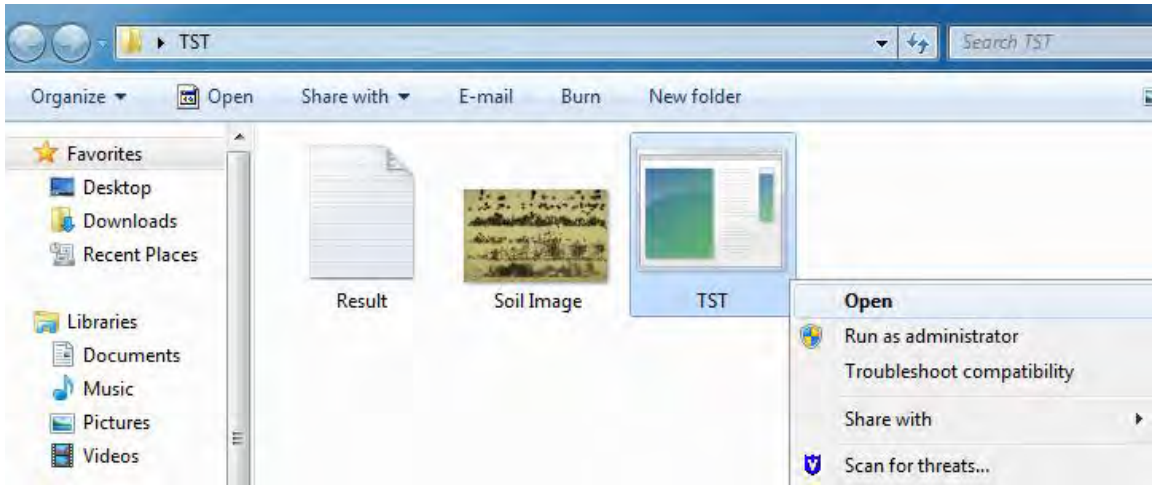

29 Opening < TST.exe > by right-clicking and selecting *Open* or by double-clicking the file.

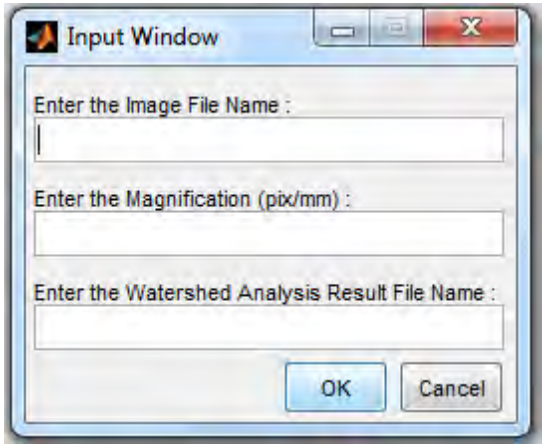

30 Inputting soil and image information into the TST computer program.

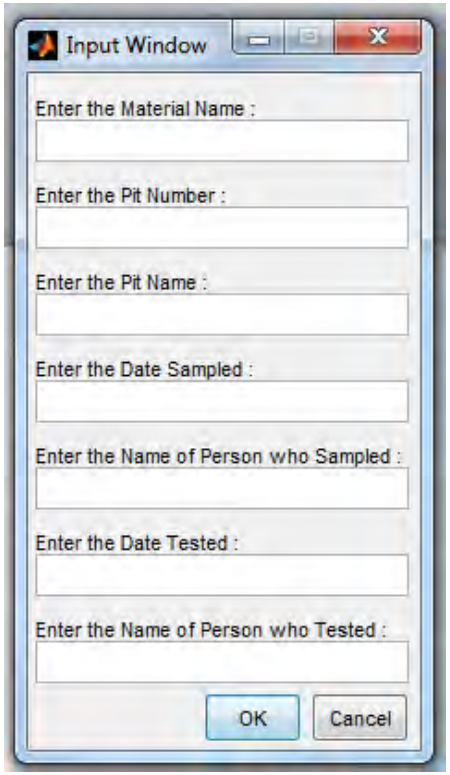

Fig. 11.11 Opening the TST program and inputting soil and image information.

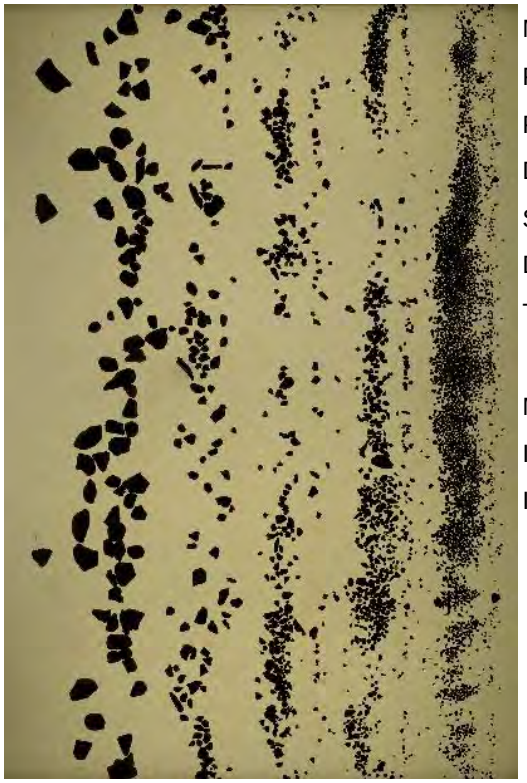

MATERIAL:

PIT NUMBER:

PIT NAME:

DATE SAMPLED:

SAMPLED BY:

DATE TESTED:

TESTED BY:

MAGNIFICATION (pix/mm): 5.7

IMAGE SIZE (pix): 3264 x 4928

IMAGE SIZE (mm): 572.6 x 864.6

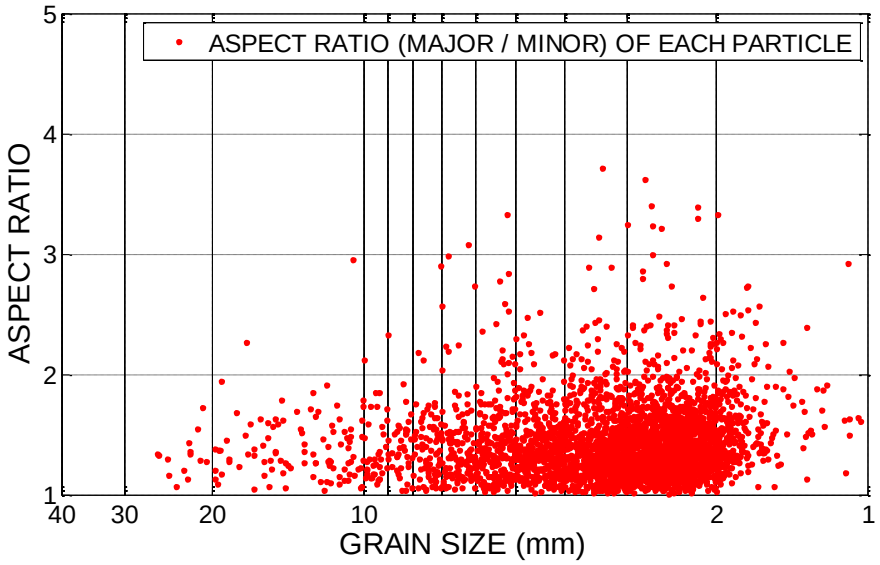

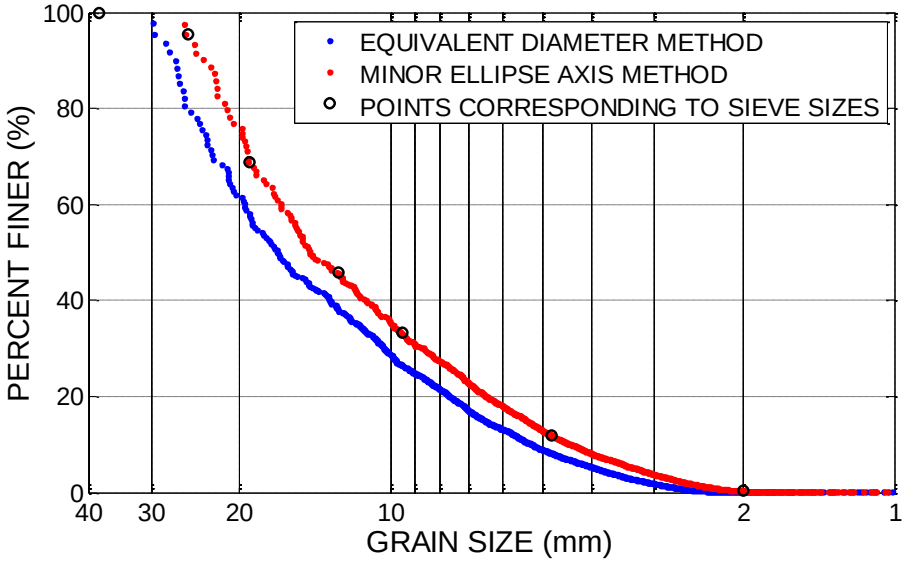

31 TST image, grain size distribution and aspect ratio for each particle

Fig. 11.12 Viewing and printing the TST test results.

MATERIAL	PIT NUMBER	PIT NAME

DATE SAMPLED	SAMPLED BY	DATE TESTED	TESTED BY

	RETAINED WEIGHT	FRACTIONAL % RETAINED	CUMULATIVE % RETAINED	RESULTS % PASSING
1 1/2 INCH	0	0	0	100
1 INCH	0	4.6671	4.6671	95.3329
3/4 INCH	0	26.5673	31.2345	68.7655
1/2 INCH	0	22.9106	54.1450	45.8550
3/8 INCH	0	12.6675	66.8126	33.1874
NO. 4	0	21.3532	88.1658	11.8342
NO. 10	0	11.5557	99.7215	0.2785

32 Table of Fractioned % Retained, Cumulative % Retained and Results % Passing

Fig. 11.13 Tabular printout of TST test results.

12. Combining Sedimaging and TST Test Results

For soils containing particles both finer and coarser than 2 mm, both the Sedimaging and TST tests are performed. Just as with the sieve-hydrometer combination, the Sedimaging and TST results must be combined. As shown in Figure 12.1, this requires knowledge of the percent passing the No. 10 (2 mm opening) sieve. If this is known, the individual results from both tests can be scaled accordingly to create the composite size distribution curve.

Several approaches were considered for determining the % finer than 2 mm. The simplest approach utilizes traditional weight measurement. The nominal specimen sizes for individual Sedimaging and TST tests are 450 grams and 1000 grams respectively. However, as mentioned in Section 11, the results of any number of TST tests may be combined to produce a single size distribution. A No. 10 (2 mm) sieve and pan are used to separate the two soil parts until either 450 grams of minus 2 mm particles or 1000 grams of plus 2 mm particles are collected. When this occurs, both fractions are weighed and their respective percentages of the total are easily computed. Additional soil is then sieved to make up the weight requirement of the other component.

If the weight fraction of the plus 2 mm soil is very small compared to the minus 2 mm fraction it may be impractical and unnecessary to use the TST device. The distribution of sizes in this case can be quickly determined by hand sieving and weighing.

A computer program “SED-TST.exe” combines both the SEDIMAGING.exe and TST.exe programs into one with only one additional input window which requests the weights of the plus 2 mm size fraction and the minus 2 mm size fraction. An example result showing the program output is included in Appendix E. The output includes a seamless grain size distribution and table of test results from both tests combined.

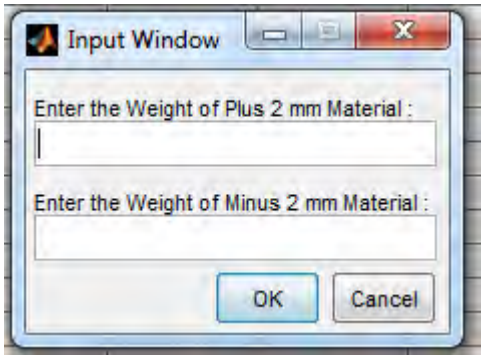

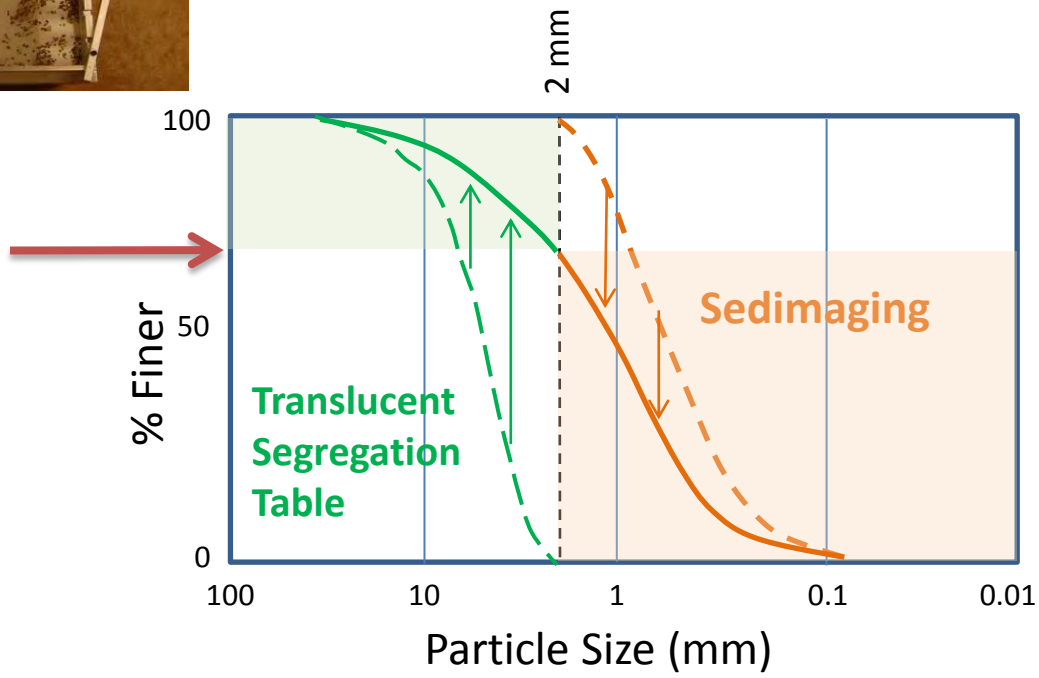

Fig. 12.1 Combining Translucent Segregation Table (TST) & Sedimaging

13. DISCUSSION OF RESULTS

This section contains an evaluation of both imaging systems in the following categories: hardware, robustness of image processing (i.e. test results), software, costs and testing times. The discussion forms the basis and leads directly to recommendations for further study in Section 15.

SEDIMAGING

Hardware

The Sedimaging research benefitted from a precipitous decrease in the costs of digital cameras during the 2nd Quarter of the project. At a $1300 cost for the body and $700 for an exceptional Nikkor macro lens, the 16.2 megapixel Nikon D 7000 strikes a perfect balance between cost and performance. The camera reduced the sedimaging testing time by over 70% since the entire soil column could now be captured with a single image at a sufficiently high resolution to characterize particles from 2.0 mm to 0.075 mm. Cameras available at the beginning of this study cost twice as much and required the capture of several images to create a stitched composite of the soil column. Since a single image could be used it could now be taken from a fixed camera position thus eliminating the need for an expensive vertical positioning system. The cost of this camera will continue to fall as even higher resolution cameras come to market.

The sedimentation column was completely redesigned during the project. It is now much easier to assemble, position, disassemble and transport. Its length was reduced from 8 ft. to 7 ft. without observable changes in test results. Further shortening may be possible. A pre-segregation system was designed which introduces the soil into the sedimentation column already somewhat segregated by size. The sediment accumulator easily connects and disconnects from the bottom of the permanently suspended sedimentation column. A connector between the sedimentation column and accumulator contains a drainage valve to empty water from the column; this allows for the determination of the percentage of fines in a specimen.

While the hardware functions reliably, it is somewhat overdesigned. The mass of aluminum used for the sedimentation column support tower, the base and the camera support column could be reduced. Material costs would be reduced with the lighter components.

Image Processing (test results)

The effectiveness of the sedimaging test must be evaluated first and foremost by its ability to duplicate or simulate sieving results. The overwhelming reason for why the results may not agree would be in the advanced image processing method based on wavelet analysis. Unlike the TST test, the particle sizes are not obtained deterministically, but rather based on analysis of image textures and calibration of these textures against sieve-determined particle sizes for many soils. As such, an unusual soil may not adhere to the "typical" or "normal" calibration which is based predominantly on multi-colored soil grains, subrounded to subangular particle shapes and uniform surface colors of individual particles.

Sedimaging tests were performed on 10 soils to compare size distributions by sedimaging to sieving. Computer outputs, tabulated results and comparisons to sieve test results are included in Appendix C. The test results are summarized in Table 13.1. For each soil the following information is tabulated:

a) Soil name
b) Date of testing
c) Dominant soil color (based on overall visual observation)
d) Color uniformity (differences in colors between particles)
e) Individual particle color uniformity (uniformity in color within individual grains)
f) Particle shape (angularity based on visual observation of images)
g) D_{60}, D_{30}, D_{10}. Coefficient of Uniformity (C_u) and Coefficient of Gradation (C_g) based on sedimaging results.
h) Image magnification
i) Height of the sedimented soil column
j) Calibration curve used in the sedimaging.exe program.
k) Horizontal spread in particle sizes at the same elevations.

The following observations are made from Table 13.1 and Appendix C:

1. Overall, the sedimaging results approximate sieving results.
2. The normal calibration curve with T=0 in equation (2.1) was used successfully for 8 of the 10 specimens. Only the 30A specimen (Test No. 3), a slag material, required T=0.25 in equation 2.1 and only the very dark and angular soil derived from gabbro rock (Specimen No. 8) required a completely unique calibration.

3. The spread in particle sizes at fixed elevations in the column ("Horizontal Spread" in Table 13.1) is an indicator of the degree of particle segregation achieved by the sedimentation column. This, in turn, may be an indicator of the uniformity of particle specific gravities in the specimen. Only 1 of the 10 specimens showed a very broad range of particle sizes at fixed elevations. Not surprisingly, this was the gabbro soil (Specimen No. 8) which, along with the following point, explains why this soil required its own calibration.
4. Individual particle color uniformity is an extremely important factor in determining if a soil will adhere to the normal calibration curve with T=0. Only two soils, the 30A (Specimen No. 3) and the Gabbro soil (Specimen No. 8) contained particles with non-uniform mottled colors. This again explains why these two soils could not use the common calibration curve with T=0.
5. It is noted that the same two unusual soils (Specimens 3 and 8) were also the only two angular materials. However, it is not believed that particle angularity itself could be the reason for departure from the normal calibration curve. The mottled colors and poor segregation are much more likely explanations.

Statistical Comparison of Sedimaging to Sieving Results

Towards the end of the project period, 20 Sedimaging tests were added to the scope of the study. These tests were performed to provide a statistical comparison to 20 parallel sieve tests conducted by MDOT on specimens split from the sedimaging specimens. The results of the blind tests performed by the University of Michigan and comparison of results to the parallel sieve tests performed by MDOT are included in Appendix F. The first 10 tests samples (Nos. 1 to 10) were made by splitting one large sample of 2NS into ten portions and putting each portion once through a sample splitter. One half was sent to UM for Sedimaging, the other was tested by MDOT. Test samples 11 through 20 were made to specific gradations after having pre-sieved a large amount of the 2NS soil. Two samples with identical gradations were prepared, one for sieving and one for Sedimaging.

The second page of the Appendix tabulates the results of the 20 Sedimaging test in terms of the equivalent "Sieve Passing Percentages" for 11 sieves. Pages 3 and 4 of Appendix F were obtained from MDOT. Here, the "Percentages Passing" from the MDOT sieve tests are compared to the Sedimaging data at 5 common sieves (Nos. 16, 30, 50, 100 and 200). The remaining 20 pages of the appendix includes two pages for each test: the usual Sedimaging results page and a page which graphically compares

Sedimaging particle size distribution curves to those by sieving. It should be noted that each of the latter pages contains not only the MDOT sieve results but also the results of sieve tests performed at UM on the exact sample that was also tested by Sedimaging. The Sedimaging tests were performed first. The sample was then dried and sieved.

The results of the first 10 tests were consistent. A good match between Sedimaging and sieving was observed for the coarser 80% of each specimen. However, the finest 20% of the material was observed to be coarser by Sedimaging than by sieving. Notwithstanding the Sedimaging results, it is particularly noteworthy that the MDOT and UM sieving results consistently disagreed on the % Passing the No. 30 sieve. UM's % passing the No. 30 sieve consistently agreed with Sedimaging results while MDOT's ranged from 6.1% to 9.4% higher. The authors do not have an explanation for this discrepancy regarding the #30 sieve. There was no such large disagreement between UM and MDOT sieve tests for the other sieve sizes.

The agreement between Sedimaging and sieving results was significantly better for the "engineered" samples (11 to 20), particularly in the finer particle size range. However, significant differences were again observed between the MDOT and UM sieving results. The UM sieve results generally matched Sedimaging results better than MDOT's sieve data did. As with tests 1-10, UM sieve tests on Samples 11-20 were performed on the same soil that was tested by Sedimaging.

Software and Computer

The sedimaging.exe program is user friendly and there is a very short learning curve. However, the computational demands are serious and 64 bit computer running under Windows 7 is required to perform the analysis. There is one potential source of operator error in the data reduction procedure: a technician must manually crop each image. If this is done carelessly, the test results could be affected. To this end, a good 24 inch monitor is essential to provide a large view of the image which would allow the operator to crop the image as close to the top and bottom of the soil column as possible.

Costs and Testing Time

The overall per unit cost of a sedimaging system is still difficult to determine as it would depend greatly on the number of units manufactured at one time. Furthermore, some savings are still expected in materials as discussed earlier in this section. The major cost is still currently the camera and lens at approximately $2000 but this price will be falling with time. Sixty four bit computers are now commonplace. Windows 7

requires this architecture. Overall, the price of the system, excluding computer is estimated at between $10,000 and $15,000.

Excluding the time to initially dry a specimen, the sedimaging test takes under 15 minutes to perform. A second drying is unnecessary. If a soil specimen does not contain fines or if their percentage does not need to be determined the sedimaging test would not even require initial drying and no specimen weight measurements would be needed. This would reduce the testing time to approximately 10 minutes.

TRANSLUCENT SEGREGATION TABLE (TST)

Hardware

The TST utilizes the same Nikon D7000 camera body and 60 mm Nikkor lens as the sedimaging system. As such, all previous discussions regarding it apply here as well. It is strongly recommended that the sedimaging and TST systems have dedicated cameras. Using one camera for both systems is unpractical because of the different set-ups and calibrations.

The remaining TST hardware is somewhat simpler than the sedimaging hardware. It is easier to manufacturer and less material is needed with the exception of the relatively large translucent and transparent plexiglass pieces. Some modifications and improvements to the system could still be made as will be discussed in Section 15 but the basic design is sound.

Image Processing (test results)

Unlike in Sedimaging, the image processing approach for the TST is deterministic. That is, the actual particle sizes are determined for every individual particle. Therefore, no calibration is needed. The key to the TST method is watershed segmentation which allows particles to be touching each other when imaged. As discussed elsewhere in this report, some differences between the TS and sieving results should be anticipated because the two tests measure different particle dimensions. More discussion on this topic follows later in this section.

The ability to the TST to determine both the minor and major axis dimensions of particles holds great promise for very rapidly characterizing the shape of numerous particles simultaneously without the use of calipers. Most importantly, this would

occur while simultaneously obtaining their overall aggregate size distribution. Section 15 will discuss how this can be accomplished.

Although TST test results have shown very good agreement with sieving, possible errors associated with extremely long particles (aspect ratios greater than 3) have not been fully evaluated. There is some evidence which shows that such particles will occasionally be interpreted by watershed segmentation as being two different particles. While the effect on size distribution would be statistically minimal, the effect on particle aspect ratio distribution could be more significant and should be explored.

Statistical Comparison of TST to Sieving Results

Just as with the Sedimaging test, 20 TST tests were added to the scope of the study. These tests were performed to provide a statistical comparison to 20 parallel sieve tests conducted by MDOT on specimens split from the TST specimens. The results of the blind tests performed by the University of Michigan and comparison of results to the parallel sieve tests performed by MDOT are included in Appendix G (TST). The first 10 tests samples (Nos. 1 to 10) were made by splitting one large sample into ten portions and putting each portion once through a sample splitter. One half was sent to UM for TST testing, the other was tested by MDOT. Test samples 11 through 20 were made to specific gradations. Two samples with identical gradations were prepared, one for sieving and one for Sedimaging.

The second page of Appendix G tabulates the results of the 20 TST tests in terms of the equivalent "Sieve Passing Percentages". Pages 3 and 4 of Appendix G were obtained from MDOT. Here, the "Percentages Passing" from the MDOT sieve tests are compared to the TST data at 5 common sieves (1", ¾" ½", 3/8" and Nos. 4 and 8). The remaining 20 pages of Appendix G include two pages per test: the TST results page and a page which compares TST particle size distribution curves to those by sieving.

Both the tabulated results and the graphical comparisons of TST particle size distributions to sieving show a clear trend of the TST slightly overpredicting particle sizes compared to the sieve definition of particle size. While the TST and sieving particle size distribution curves generally paralleled each other, consistent offsets of the TST curves to the coarser side were observed. The reason for this offset is strongly believed to be the result of having not accounted for all three particle dimensions when computing particle weights/volumes in the TST test. As discussed in Section 7, with reference to Figure 7.2, the TST particle size is defined by the smaller particle dimension in the cameras view. This remains a logical and valid assumption. However, when computing

the particle volumes, since the particle dimension in the vertical direction (axis towards the camera) cannot be determined from the image, this third dimension was assumed to be the same as the same smaller dimension observed by the camera. In other words, two of the three particle dimensions were assumed to be the same smaller dimension of a best-fitting ellipse in the cameras view of the particle. However, the third (vertical) dimension should generally be even smaller than the smaller dimension observed in the planer view. To rectify this uncertainty, the bridge underpass heights can be used to estimate the third (vertical) dimension. Early results not presented in this report support the hypothesis that when all three dimensions are accounted for (2 obtained from the camera image and 1 from a particles final location on the table) the TST results will match the sieve-defined particle size distributions much better. In fact, some indications are that they will match almost perfectly.

Software and Computer

The TST software is very robust. It utilizes *ImageJ* to perform the image thresholding, watershed segmentation and size analysis. The results are imported into TST.exe which produces the computer output. The TST test may utlize the same 64-bit computer as is needed for sedimaging.

Costs and Testing Time

Even with a dedicated Nikon D7000, the cost of a TST system should be under $10,000. The TST test takes less than 10 minutes to perform per 1.2 kg of specimen. For specimens exceeding about 1.2 kg, approximately 8 additional minutes are needed since the test has to be performed twice (16 minutes are needed for specimens exceeding about 2.4 kg, etc.).

Table 13.1 Summary of Sedimaging Test Results

No.	Soil Name	Test Date	Color		Individual Particle Color Uniformity	Shape	D_{60} (mm)	D_{30} (mm)	D_{10} (mm)	C_u Coef. of Unif.	C_g Coef. of Grad.	Calibration Curve Used	Horizontal Spread
			Dominant	Uniformity Between Particles									
1	2 NS w/o fines	04/18/11	light brown	no	uniform	subrounded to subangular	0.45	0.30	0.20	2.21	1.00	common (T=0)	normal
2	Griffin, IN w/o fines	04/22/11	light brown	no	uniform	subrounded to subangular	0.67	0.45	0.34	1.94	0.88	common (T=0)	normal
3	30A w/o fines	04/23/11	light brown	no	mottled, irregular	angular	0.53	0.27	0.15	3.46	0.89	common (T=0.25)	very narrow
4	Oakland Co. w/o fines	04/25/11	light brown	yes	uniform	subangular	0.37	0.24	0.19	1.90	0.84	common (T=0)	normal
5	Costa Rica w/o fines	04/30/11	black	no	uniform	subrounded	0.16	0.12	0.11	1.49	0.91	common (T=0)	narrow
6	Upper Peninsula w/o fines	05/08/11	reddish	no	somewhat uniform	subrounded to subangular	0.58	0.31	0.20	2.88	0.85	common (T=0)	normal
7	2 NS w fines added	05/26/11	light brown	no	uniform	subrounded to subangular	0.33	0.14	NA	NA	NA	common (T=0)	narrow
8	Gabbro soil w/o fines	05/26/11	black	yes	mottled	angular	0.77	0.46	0.26	2.98	1.06	soil specific	very broad
9	Class IIA w/ fines	08/26/11	v. light brown	no	uniform	subangular	0.22	0.15	0.11	2.04	0.94	common (T=0)	normal
10	Upper Peninsula w/ fines	08/30/11	reddish	no	somewhat uniform	subrounded to subangular	0.32	0.20	NA	NA	NA	common (T=0)	normal

14. CONCLUSIONS

1. This research demonstrated the feasibility of digital imaging technology as a viable alternative to traditional sieving for determination of soil and aggregate size distributions. Digital imaging is less expensive and faster than sieving while producing similar results.

2. Because of the large range of soil and aggregate particle sizes, no single image-based method could be developed to size all particles from U .S. Standard Sieve No. 200 (0.075 mm) to 1 in. and larger.

3. For particles finer than the No. 10 Standard U.S. Sieve (2 mm), a method hereby termed "sedimaging" was developed. Unlike the deterministic TST approach, the sedimaging method relies on statistical interpretation of image textures. The soil specimen is sedimented through a 4 in. x 4 in. x 7 ft. long water-filled column to segregate it by size. The sedimented soil is photographed through a glass window in a sediment accumulator attached to the bottom of the sedimentation column. The image of the sedimented soil is then incrementally analyzed to generate some 5,000 data points (particle sizes), each representing a 128 pix. x 128 pix region of the image. The image processing requires a calibration between an image "wavelet index" and the average pixel size in units of image pixels. The test takes 15 minutes if the percentage of fines is to be determined or 10 minutes if the percentage of fines is not needed. In the latter case, the soil does not have to be dried and no specimen weights need to be recorded. Tests on 10 different soils with varying soil colors, textures and gradations have yielded results approximating sieving results.

4. A deterministic method using an inclining 3 ft. x 3 ft. translucent segregation table (TST) with a ceiling-mounted camera was developed for particles larger than the No. 10 Standard U.S. Sieve (2 mm). The soil specimen is "brushed" down the inclined plane while passing beneath a series of bridges with decreasing underpass heights in order to somewhat segregate the particles by size. The segregation is necessary to keep smaller particles from hiding from view beneath larger particles. The translucent table is backlit to help threshold the images. An image processing method called "watershed segmentation" is used to digitally separate touching particles. In the TST test, the size and aspect ratio of every individual particle is determined. The test takes approximately 10 minutes to perform and requires no measurements of specimen weight. Based on a small number of samples to date, test results have been very good and will undoubtedly become even better when the third (vertical) particle dimension is estimated from the TST bridge heights.

5. For specimens containing particles both coarser and finer than the No.10 Standard U.S. Sieve, both the sedimaging and TST tests are performed for the finer and coarser fractions respectively. The only additional information to be recorded is the relative percentage of the soil particles coarser and finer than the No. 10 sieve.

6. Both the sedimaging and TST tests utilize 16.2 megapixel Nikon D7000 cameras with 60 mm macro Nikkor lenses. The cameras are controlled remotely from a 16-bit computer running a program called NKRemote by Breeze Software. User-friendly software has been written for both tests. The programs are appropriately called Sedimaging.exe and TST.exe and were written in the MATLAB environment. They require minimum operator input, perform all of the image processing and print the results to files or a printer. For specimens requiring both the sedimaging and TST tests, a composite program called Sed-TST.exe is used.

7. A statistical comparison was made of particle size distributions determined by the two image-based tests and by sieving. Twenty Sedimaging and 20 TST tests were performed at the University of Michigan while the forty sieving tests on split samples was performed by MDOT.

   For the Sedimaging test, some deviations from sieving results were observed for the fine sand fractions of almost every test. However, the overall results correlated with the curious exception of "% passing the No. 30 sieve". No explanation for this discrepancy has been found. However, when additional sieve tests were conducted at UM on the very same 20 samples that were tested by Sedimaging, the "% passing the No. 30 sieve" agreed very well with Sedimaging results.

   The statistical differences between the 20 TST results and MDOT's sieve tests was more significant. However, the source of the discrepancy is strongly believed to be in the algorithm used to compute particle volumes by the TST. The TST test results presented in Appendix G only accounted for the two particle dimensions in the camera's field of view. When the third (vertical) dimension is included in the computation, the results will much better agree with sieving.

   Based on the statistical analysis performed it was concluded that the Sedimaging and TST tests could not yet be considered as an alternative to sieving for MDOT acceptance testing. However, as described above, the issues that caused the discrepancies in results may shortly be overcome. At this time, both the TST and Sedimaging tests appear to be viable methods for particle size assessment in aggregate production.

15. RECOMMENDATIONS FOR FURTHER RESEARCH

1. The TST System holds great promise for completely describing the three-dimensional shape of aggregates. The TST.exe program presently yields the longer and intermediate dimension of every particle. The third (vertical) dimension, typically the smallest, cannot be determined from the overhead images. However, this third dimension can be bracketed by the underpass heights of the two bridges between which the particles come to rest. Some modifications to the TST hardware will be needed to insure uniform underpass heights and the software will have to be updated to include this potential new feature of the TST. Once the third dimension becomes determinable, discrepancies between TST tests and sieving, such as were observed in MDOT's statistical testing (Appendix G) may be eliminated.

   Present methods of determining aggregate sizes rely on manual measurements with calipers, one particle at a time. Therefore, the modified TST test could greatly reduce or completely eliminate the need for such laborious efforts.

2. Related to recommendation #1, the watershed segmentation method may need to be modified as it appears that some elongated particles are interpreted as being two particles and therefore as having a smaller aspect ratio than they actually have.

3. As the price of digital cameras continues to drop, consideration may be given to design of a larger TST which would accommodate larger specimens. A 48 in. x 48 in. table could handle a 2.5 kg of aggregate. However, such a table would require a 30 megapixel camera. Fortuitously, in 2012 Nikon will introduce a 32 megapixel camera at a cost of only $3,000.

4. The success of the TST suggests that its range of applicability could be pushed to finer particles, say 1.19 mm (Standard U.S. Sieve No. 16). However, this too would require a higher resolution camera. If the TST could accommodate particles down to 1.19 mm, the sedimaging test hardware demands could be greatly reduced. The sedimentation column and accumulator could be as small as 1.25 in. x 1.25 in. x 5 ft. and could cost much less to construct than using the current design.

5. Even if the sedimentation system is not scaled down it can nevertheless be redesigned to have lighter components. As discussed in Section 13, while the hardware functions efficiently and reliably, it is somewhat overdesigned. The mass of

aluminum used for the sedimentation column support tower, the base and the camera support column could all be reduced.

6. Related to recommendation #4, the current U.S. Standard Sieve No. 10 (2.00 mm) criteria does not correspond to a standard sieve number commonly used by MDOT and therefore makes the separation of particles for the two tests somewhat unnatural. Either U.S. Standard Sieve No. 8 (2.38 mm openings) or preferably the U.S. Standard Sieve No.16 (1.19 mm openings) should be established as the break between the two tests.

7. A wider range of soil types need to be investigated in the sedimaging test to establish if the "Common *T*=0" calibration curve will continue to be useful for the majority of soils encountered in Michigan.

8. The sedimaging test occasionally appears to underestimate the equivalent percentage loss by wash (particles finer than the No. 200 sieve). This may be because insufficient time has been given for the specimen to soak prior to pre-segregation. In addition to extra time for soaking, consideration should be given to decanting "dirty" water from the pre-segregation tube once or twice before introducing the specimen into the sedimentation column. The presence of trace low specific gravity particles including organic debris, mica flakes and shale particles can also result in underestiamation of the finer soil particles because such particles settle within the matrix of the finer soil. Consideration should be given to methods for removal of such low density fragments.

16. RECOMMENDATIONS FOR IMPLEMENTATION

The following recommendations for implementation were developed by MDOT Project Manager and supported by the authors of the report.

1. Communicate the feasibility of digital imaging of earth materials to other state DOT's and federal agencies.

2. Support additional research at the national level for a robust statistical study comparing sedimaging and TST to traditional sieve testing.

3. Encourage the development of nationally recognized test methods (e.g. ASTM and AASHTO) when equivalency to sieve testing is statistically supported.

4. Encourage aggregate producers to support research and experiment with digital imaging technologies to lower testing costs and/or improve quality control.

APPENDIX A

BIBLIOGRAPHY

Al-Rousan, Masad, E., Tutumluer, E., and Pan, T. (2007). "Evaluation of Image Analysis Techniques for Quantifying Aggregate Shape Characteristics." Construction and Building Materials, 21, 978-990.

Al-Rousan, T., Masad, E., Myers, L., and Speigelman, C. (2005). "New Methodology for Shape Classification of Aggregates." Transportation Research Record, 1913, 11-23.

Alshibli, K. A. and Alsaleh, M. I. (2004). "Characterizing Surface Roughness and Shape of Sands Using Digital Microscopy." Journal of Computing in Civil Engineering, 18(1), 36-45.

Alshibli, K. A., Macari, E. J., and Sture, S. (1996). "Digital Imaging Techniques for Assessment of Homogeneity of Granular Materials." Transportation Research Record, 1526, 121-128.

Bareither, C. A., Edil, T. B., Benson, C. H., and Mickelson, D. M. (2008). "Geological and Physical Factors Affecting the Friction Angle of Compacted Sands." Journal of Geotechnical and Geoenvironmental Engineering, 134(10), 1476-1489.

Barrett, P. J. (1980). "The Shape of Rock Particles: A Critical Review." Sedimentology, 27(), 291-303.

Bowman, E. T. (2002). "Ageing and Creep of Dense Granular Materials." Ph. D. Thesis, University of Cambridge.

Bowman, E. T. and Soga, K. (2003). "Creep, Ageing and Microstructural Change in Dense Granular Materials." Soils and Foundations, 43(4), 107-117.

Bowman, E. T., Soga, K., and Drummond, W. (2001). "Particle Shape Characterisation Using Fourier Descriptor Analysis." Géotechnique, 51(6), 545-554.

Brzezicki, J. M. and Kasperkiewicz, J. (1999). "Automatic Image Analysis in Evaluation of Aggregate Shape." Journal of Computing in Civil Engineering, 13(2), 123-128.

Canny, J. (1986). “A computational approach to edge detection.” IEEE Trans. Pattern Anal. and Machine Intelligence, 8(6), 679-698.

Chandan, C., Sivakumar, K., Masad, E., and Fletcher, T. (2004). "Application of Imaging Techniques to Geometry Analysis of Aggregate Particles." Journal of Computing in Civil Engineering, 18(1), 75-82.

Cho, G. C., Dodds, J, and Santamarina, J. C. (2006). "Particle Shape Effects on Packing Density, Stiffness, and Strength: Natural and Crushed Sands." Journal of Geotechnical and Geoenvironmental Engineering, 132(5), 591-602.

Das, N., Thomas, S., Kopmann, J, Donovan, C., Hurt, C., Daouadji, Al, Ashmawy, A. K., and Sukumaran, B. (2011). "Modeling Granular Particle Shape Using Discrete Element Method." Geo-Frontiers 2011, 4293-4302.

Davies, E.R. (2005) Machine Vision, 3rd ed. Morgan Kaufmann Publishers - Elsevier Inc., 934 pp.

Devaux, M.F., Robert, P., Melcion, J.P. Le Deschault de Monredon, F. (1997) “Particle Size of Bulk Powders using Mathematical Morphology”, Powder Technology, 90(1997), pp. 141-147.

Dodds, J. (2003). "Particle Shape and Stiffness - Effects on Soil Behaviour." Master's Thesis, Georgia Institute of Technology.

Fletcher, T., Chandan, C., Masad, E., and Sivakumar, K. (2003). "Aggregate Imaging System for Characterizing the Shape of Fine and Coarse Aggregates." Transportation Research Record, 1832, 67-77.

Fletcher, T., Chandan, C., Masad, E., and Sivakumar, K. (2002). "Measurement of Aggregate Texture and its Influence on Hot Mix Asphalt (HMA) Permanent Deformation." Journal of Testing and Evaluation, 30(6), 524-531.

Ghalib, A.M. and Hryciw, R.D. (1999) "Soil Particle Size Distribution by Mosaic Imaging and Watershed Analysis," Journal of Computing in Civil Engineering, Vol. 13, No. 2, pp. 80-87.

Ghalib, A.M., Hryciw, R.D. and Shin, S.C. (1998) "Image Texture Analysis and Neural Network for the Characterization of Uniform Soils," Proc., ASCE Congress on Computing in Civil Engineering, pp. 671-682.

Graham, D. J., Reid, I., and Rice, S. P. (2005). "Automated sizing of coarse-grained sediments." Mathematical Geology, 37(1), 1-28.

Haralick, R.M., Shanmugam, K., and Dinstein, I. (1973) "Textural Features for Image Classification", IEEE Transactions on Systems, Man and Cybernetics, SMC-3(6), pp. 610-621.

Harr, A. (1910) "Zur Theorie der Orthogonalen Function en Systeme," Math. Annal., 69, pp. 331-371.

Hryciw, R.D. and Jung, Y. (2009) "Three Point Imaging Test for AASHTO Soil Classification", Transportation Research Record, the Journal of the Transportation Research Board, No. 2101, pp. 27-33.

Hryciw, R.D. and Jung, Y. (2008) "Accounting for Void Ratio Variation in Determination of Grain Size Distribution by Soil Column Image Processing", Geotechnical Special Publication 179, Characterization, Monitoring, and Modeling of GeoSystems, Proc. of ASCE GeoInstitute GeoCongress, New Orleans, pp. 966-973.

Hryciw, R.D., Jung, Y. and Susila, E. (2008) "Characterization of Thin Layers in Soil Stratigraphies by VisCPT and FEM Simulations with Adaptive Remeshing", Proc. of the 2008 NSF Engineering Research and Innovation Conference, Knoxville, TN. 8 pp.

Hryciw, R.D., Shin, S. and Ghalib, A.M. (2003) "High Resolution Site Characterization by VisCPT with Application to Hydrogeology", Proc. of Soil and Rock America, the 12th Panamerican Conference on Soil Mechanics and Geotechnical Engineering, Vol. 1, pp. 293-298.

Hryciw, R.D., Ghalib, A. M. and Raschke, S. A. (1998) "In-Situ Soil Characterization by VisCPT", Proceedings of the First International Conference on Site Characterization (ISC'98), Balkema Press, pp. 1081-1086.

Hryciw, R.D., Ghalib, A.M. and Raschke, S.A. (1998) "Methods for Soil Characterization from Images of Grain Assemblies", Proceedings of the 2nd International Conference on Imaging Technologies: Techniques and Applications in Civil Engineering ", ASCE, pp. 88-99.

Hryciw, R.D., Raschke, S.A. and Ghalib, A.M. (1997) "Characterization of Particulate Assemblies Through Computer Vision", in *Selected Research in Environmental Quality*, Proc. of a Joint USAF/Army Contractor/Grantee Meeting, Jan. 14-17, Panama City, FL. , pp. 131-136.

Hryciw, R.D. and Raschke, S.A. and (1996) "Development of Computer Vision technique for In-Situ Soil Characterization" in *Emerging Technologies in Geotechnical Engineering*, Transportation Research Record No. 1526, pp. 86-97.

Hryciw, R. D., Shin, S., Jung, Y. (2006) “Soil Image Processing – Single Grains to Particle Assemblies” CD Proceedings of *Geotechnical Engineering In the Information Technology Age*, ASCE GeoInstitute GeoCongress, Atlanta, GA. 6 pp.

Jung, Y. and Hryciw, R. D. (2011) “Particle Size Distribution by Sedimentation and Image Analysis” submitted to the ASTM Geotechnical Testing Journal.

Jung, Y. and Hryciw, R.D. (2011) “Image Edge Pixel Density (EPD) Model for Soil Grain Size”, submitted to the ASCE Journal of Computing in Civil Engineering.

Jung, Y. and Hryciw, R. D., Elsworth, D. (2008) “Vision Cone Penetrometer Calibration for Soil Grain Size”, Geotechnical and Geophysical Site Characterization, Proceedings of the Third International Conference on Site Characterization ISC’3, Taipei, Taiwan, Taylor & Francis, pp. 1303-1308.

Kass, M., Witkin, A., and Terzopoulos, D., (1987) “Active Contour Models,” International Journal of Computer Vision, 1(4), pp. 321-331.

Kim, H., Haas, C. T., Rauch, A. F., and Browne, C. (2002). "Wavelet-Based Three-Dimensional Descriptors of Aggregate Particles." Transportation Research Record, 1787, 109-116.

Krumbein, W. C. and Sloss, L. L. (1963). "Stratigraphy and Sedimentation." W. H. Freeman and Company, San Francisco.

Kuo, C. -Y. (2002). "Correlating Permanent Deformation Characteristics of Hot Mix Asphalt with Aggregate Geometric Irregularities." Journal of Testing and Evaluation, 30(2), 136-144.

Kuo, C. -Y. and Freeman, R. B. (2000). "Imaging Indices for Quantification of Shape, Angularity, and Surface Texture of Aggregates." Transportation Research Record, 1721, 57-65.

Kuo, C. -Y. and Freeman, R. B. (1998). "Image Analysis Evaluation of Aggregates for Asphalt Concrete Mixtures." Transportation Research Record, 1615, 65-71.

Kuo, C. -Y., Frost, J. D., Lai, J. S., and Wang, L. B. (1996). "Three-Dimensional Image Analysis of Aggregate Particles from Orthogonal Projections." Transportation Research Record, 1526, 98-103.

Kuo, C. -Y., Rollings, R. S., and Lynch, L. N. (1998). "Morphological Study of Coarse Aggregates Using Image Analysis." Journal of Materials in Civil Engineering, 10(3), 135-142.Laferty, D. (1994) “Digital Composite Imaging for High Resolution Specimen Analysis,” J.N.I.H. Res. 6, 78 pp.

Lassoued, N., Babin, P., Della Valle, G. Devaux, M.-F., Reguerre, A.-L. (2007) “Granulometry of Bread Crumb Grain: Contributions of 2D and 3D Image Analysis at Different Scale”, Food Research International, 40, pp. 1087-1097

Maerz, N. H. (2004). “Technical and computational aspects of the measurement of aggregates shape by digital image processing.” J. Comput. Civ. Eng., 18(1), 10-18.

Mahmoud, E., Gates, L., Masad, E., Erdogan, S., and Garboczi, E. (2010). "Comprehensive Evaluation of AIMS Texture, Angularity, and Dimension Measurements." Journal of Materials in Civil Engineering, 22(4), 369-379.

Mahmoud, E., Masad, E., and Nazarian, S. (2010). "Discrete Element Analysis of the Influences of Aggregate Properties and Internal Structure on Fracture in Asphalt Mixtures." Journal of Materials in Civil Engineering, 22(1), 10-20.

Marr, D. and Hildrcth, E. (1980). “Theory of edge detection.” Proc. R. Soc. London, Series B, 207, 187-217.

Masad, E., Button, J.W. and Papagiannakis, T. (2000) “Fine Aggregate Angularity: Automated Image Analysis Approach”, Transportation Research Record, No. 1721, Transportation Research Board, pp. 66-72.

Masad, E., Olcott, D., White, T., and Tashman, L. (2001). "Correlation of Fine Aggregate Imaging Shape Indices with Asphalt Mixture Performance." Transportation Research Record, 1757, 148-156.

Matheron, G. (1975) *Random Sets and Integral Geometry,* John Wiley & Sons, New York., 261pp.

Matheron, G. (1967) *Éléments Pour Une Théorie Des Milieux Poreux.* Paris: Masson et Cie, 168 pp.

Mazille, J. E. (1987). “A deagglomeration algorithm for highly coalescent particles.” Acta Stereol., 669–673.

Meloy, T. P. (1977). "Fast Fourier Transforms Applied to Shape Analysis of Particle Silhouettes to obtain Morphological Data." Powder Technology, 17, 27-35.

Mitchell, J. K. and Soga, K. (2005). "Fundamentals of Soil Behavior." John Wiley & Sons, New Jersey.

Mishra, D., Tutumluer, E., and Xiao, Y. (2010). "Particle Shape, Type and Amount of Fines, and Moisture Affecting Resilient Modulus Behavior of Unbound Aggregates." GeoShanghai 2010 International Conference, 279-287.

Nievergelt, Y. (1999) Wavelets Made Simple, Birkhauser, Boston, MA 297 pp.

Pan, T. (2002). "Fine Aggregate Characterization Using Digital Image Analysis." Master's Thesis, Louisiana State University, 1-110.

Pan, T. and Tutumluer, E. (2006). "Quantification of Coarse Aggregate Surface Texture Using Image Analysis." Journal of Testing and Evaluation, 35(2), 1-10.

Pan, T., Tutumluer, E., and Anochie-Boateng, J (2006). "Aggregate Morphology Affecting Resilient Behavior of Unbound Granular Materials." Transportation Research Record, 1952, 12-20.

Pan, T., Wang, L., and Tutumluer, E. (2011). "Experimental Investigation of Aggregate-Mortar Interface Affecting the Early Fracture Toughness of Portland Cement Concrete." Internaional Journal of Pavement Research and Technology, Chinese Society of Pavement Engineering, 4(3), 168-175.

Prodanov, D., Heeroma, J. and Marani, E. (2006) “Automatic Morphometry of Synaptic Boutons of Cultured Cells using Granulometric Analysis of Digital Images”, Journal of Neuroscience Methods, 151, pp.168-177

Qian, Y., Tutumluer, E., and Huang, H. (2011). "A Validated Discrete Element Modeling Approach for Studying Geogrid-Aggregate Reinforcement Mechanisms." Geo-Frontiers 2011, 4653-4662.

Rao, C. and Tutumluer, E. (2000). "Determination of Volume of Aggregates." Transportation Research Record, 1721, 73-80.

Rao, C., Tutumluer, E., and Kim, I. T. (2002). "Quantification of Coarse Aggregate Angularity Based on Image Analysis." Transportation Research Record, 1787, 117-124.

Rao, C., Tutumluer, E., and Stefanski, J. A. (2001). "Coarse Aggregate Shape and Size Properties Using a New Image Analyzer." Journal of Testing and Evaluation, 29(5), 461-471.

Raschke, S.A. and Hryciw, R. D. (1997a) "Soil Grain Size Distribution by Computer Vision" ASTM Geotechnical Testing Journal, Vol. 20, No. 4, pp. 433-422.

Raschke, S.A. and Hryciw, R. D. (1997b) "Vision Cone Penetrometer (VisCPT) for Direct Subsurface Soil Observation", ASCE Journal of Geotechnical and Geoenvironmental Engineering, Vol. 123, No. 11, pp. 1074-1076.

Roberts, L. (1965). Machine perception of 3-D solids, optical and electro-optical information processing, MIT Press.

Sallam, A. M. (2004). "Studies on Modeling Angular Soil Particles Using the Discrete Element Method." Ph. D. Thesis, University of South Florida.

Sallam, A. M. and Ashmawy, A. K. (2009). "Effect of Particle Shape and Angularity on Dilation of Granular Soils: A Discrete Element Approach." Proceedings of the XVII International Conference on Soil Mechanics and Geotechnial Engineering, Alexandria, Egypt.

Santamarina, J. C. and Cho, G. C. (2004). "Soil Behaviour: The Role of Particle Shape." The Skempton Conference, 74(5), 604-617.

Santamarina, J. C. and Cho, G. C. (2001). "Determination of Critical State Parameters in Sandy Soils: Simple Procedure." Geotechnical Testing Journal, 24(2), 185-192.

Serra, J. (1982) *Image Analysis and Mathematical Morphology,* Academic Press, New York, NY., 601 pp.

Shin S. and Hryciw R.D. (2004) "Application of Wavelet Analysis to Soil Mass Images for Particle Size Determination" ASCE Journal of Computing in Civil Engineeing, Vol. 18, No 1. pp. 19-27.

Sternberg, S. R. (1986) "Grayscale Morphology", Comput. Vision, Graph. Image Processing. Vol. 35., No. 3, pp. 333-355.

Sukumaran, B. and Ashmawy, A. K. (2003). "Influence of Inherent Particle Characteristics on Hopper Flow Rate." Powder Technology, 138, 46-50.

Sukumaran, B. and Ashmawy, A. K. (2001). "Quantitative Characterisation of the Geometry of Discrete Particles." Géotechnique, 51(7), 619-627.

Tutumluer, E. and Pan, T. (2008). "Aggregate Morphology Affecting Strength and Permanent Deformation Behavior of Unbound Aggregate Materials." Journal of Materials in Civil Engineering, 20(9), 617-627.

Tutumluer, E., Pan, T., and Carpenter, S. H. (2003). "Investigation of Aggregate Shape Effects on Hot Mix Performance Using an Image Analysis Approach." Report for the Federal Highway Administration, 1-249.

Tutumluer, E., Rao, C., and Stefanski, J. A. (2000). "Video Image Analysis of Aggregates." Report for the Illinois Department of Transportation, University of Illinois at Urbana-Champaign, 1-162.

Van den Berg, E. H., Meesters, A. G. C. A., Kenter, J. A. M., and Schlager, W. (2002). "Automated separation of touching grains in digital images of thin sections." Computers and Geosciences, 28(2), 179-190.

Vincent, L. (1993). "Morphological reconstruction in image analysis: applications and efficient algorithms." IEEE Trans. Image Process, 2(2), 176-201.

Wadell, H. (1932). "Volume, Shape, and Roundness of Rock Particles." Journal of Geology, 40, 443-451.

Wang, L., Lane, S., Lu, Y., and Druta, C. (2009). "Portable Image Analysis System for Characterizing Aggregate Morphology." Transportation Research Record, 2104, 3-11.

Wang, L., Wang, X., Mohammad, L., and Abadie, C. (2005). "Unified Method to Quantify Aggregate Shape Angularity and Texture Using Fourier Analysis." Journal of Materials in Civil Engineering, 17(5), 498-504.

Wettimuny, R. and Penumadu, D. (2004). "Applicatoin of Fourier Analysis to Digital Imaging for Particle Shape Analysis." Journal of Computing in Civil Engineering, 18(1), 2-9.

Wilson, J. D. and Klotz, L. D. (1996). "Quantitative Analysis of Aggregate Based on Hough Transform." Transportation Research Record, 1530, 111-115.

Wu, Y.S., van Vliet, L.J., Frijlink, H.W. van der Voort Maarschalk, K. (2007) “Pore Size Distribution in Tablets Measured with a Morphological Sieve”, International Journal of Pharmaceutics, 342, pp. 176-183.

Xiao, Y., Tutumluer, E., and Siekmeier, J. (2011). "Resilient Modulus Behavior Estimated from Aggregate Source Properties." Geo-Frontiers 2011, 4843-4852.

Xu, B., Wang, S., and Su, J. (1999). “Fiber image analysis, Part III: autonomous separation of fiber cross sections.” J. Textile Inst. 90, 288-297.

Yen, Y. K., Lin, C. L., and Miller, J. D. (1998). “Particle overlap and segregation problems in on-line coarse particle size measurement.” Powder Technol., 98(1), 1–12.

APPENDIX B.

DERIVATION OF EQUATION FOR PARTIAL PERCENTAGE OF FINES

Notation

$P\%F$ = Partial Percentage of fines

W_s = Original dry weight of soil

W_c = Weight of soil canister [known]

W_{s+c} = Weight of dry soil and canister [measured]

W_{sa} = Weight of soil in accumulator

W_a = Weight of empty accumulator [known]

W_{wf} = Final weight of water in accumulator (when soil occupies some volume).

W_{s+wf+a} = Weight of: soil in accumulator + final water in accumulator + empty accumulator [measured]

W_{w_o} = Original weight of water in accumulator (before soil is introduced).

W_{a+w} = Weight of accumulator filled with water (but no soil) [known]

Derivation

By definition, the partial percentage of fines is:

$$P\%F = \left(W_s - W_{sa}\right)/W_s \quad \text{... (1)}$$

The dry weight of soil is computed after weighing the soil + canister:

$$W_s = W_{s+c} - W_c \quad \text{... (2)}$$

The weight of soil in the accumulator would be:

$$W_{sa} = W_{s+wf+a} - W_a - W_{wf} \quad \text{... (3)}$$

The final weight of water = original weight of water - weight of water displaced by soil:

$$W_{wf} = W_{w_o} - \frac{W_{sa}}{G_s} \quad \text{... (4)}$$

where:

$$W_{w_o} = W_{a+w} - W_a \quad \text{... (5)}$$

Combining (4) and (5) into (3):

$$W_{sa} = W_{s+wf+a} - W_a - \left\lfloor W_{w_o} - \frac{W_{sa}}{G_s} \right\rfloor$$

$$W_{sa} = W_{s+wf+a} - W_a - \left\lfloor W_{a+w} - W_a - \frac{W_{sa}}{G_s} \right\rfloor$$

$$W_{sa} = W_{s+wf+a} - W_{a+w} + \frac{W_{sa}}{G_s} \quad \text{... (6)}$$

Solving Eq. (6) for W_{sa} :

$$W_{sa} - \frac{W_{sa}}{G_s} = W_{s+wf+a} - W_{a+w}$$

$$W_{sa}\left(1 - \frac{1}{G_s}\right) = W_{s+wf+a} - W_{a+w}$$

$$W_{sa} = \frac{G_s \lfloor W_{s+wf+a} - W_{a+w} \rfloor}{G_s - 1} \quad \text{... (7)}$$

For most soils $2.62 < G_s < 2.70$ in which case:

$$W_{sa} \approx 1.6 \lfloor W_{s+wf+a} - W_{a+w} \rfloor \quad \text{...(8)}$$

APPENDIX C

EXAMPLE SEDIMAGING TEST RESULTS

MATERIAL: 2NS w/o Fines

PIT NUMBER:

PIT NAME:

DATE SAMPLED: 04/18/2011

SAMPLED BY: HS

DATE TESTED: 04/18/2011

TESTED BY: HS

D_{60} (mm): 0.45

D_{30} (mm): 0.30

D_{10} (mm): 0.20

C_u: 2.21

C_g: 1.00

MAGNIFICATION (pix/mm): 35.0

IMAGE SIZE (pix): 4152 x 1280

IMAGE SIZE (mm): 118.6 x 36.6

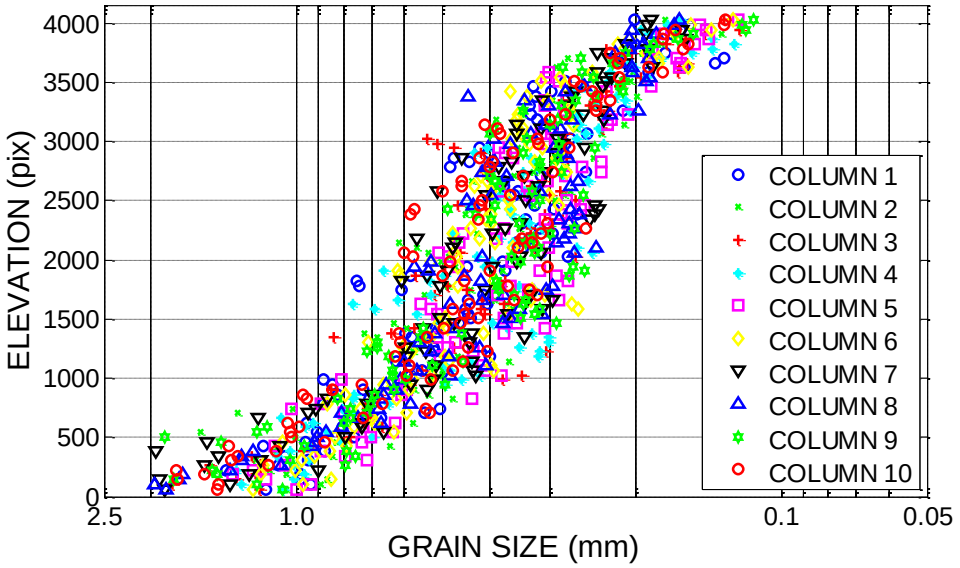

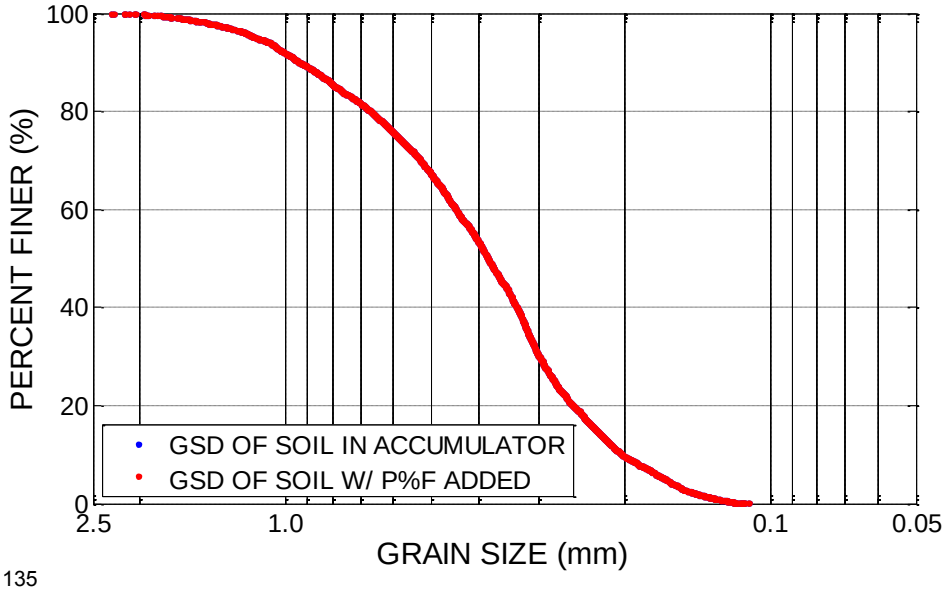

MATERIAL	PIT NUMBER	PIT NAME
2NS w/o Fines		

DATE SAMPLED	SAMPLED BY	DATE TESTED	TESTED BY
04/18/2011	HS	04/18/2011	HS

	FRACTIONAL % RETAINED	CUMULATIVE % RETAINED	RESULTS % PASSING
NO. 10	0.2000	0.2000	99.8000
NO. 20	12.3000	12.5000	87.5000
NO. 30	11.6000	24.1000	75.9000
NO. 40	18.7000	42.8000	57.2000
NO. 50	27.1000	69.9000	30.1000
NO. 60	10.9000	80.8000	19.2000
NO. 70	7.3000	88.2000	11.8000
NO. 80	4.6000	92.8000	7.2000
NO. 100	4.5000	97.3000	2.7000
NO. 200	2.7000	100	0

Material: 2NS w/o Fines

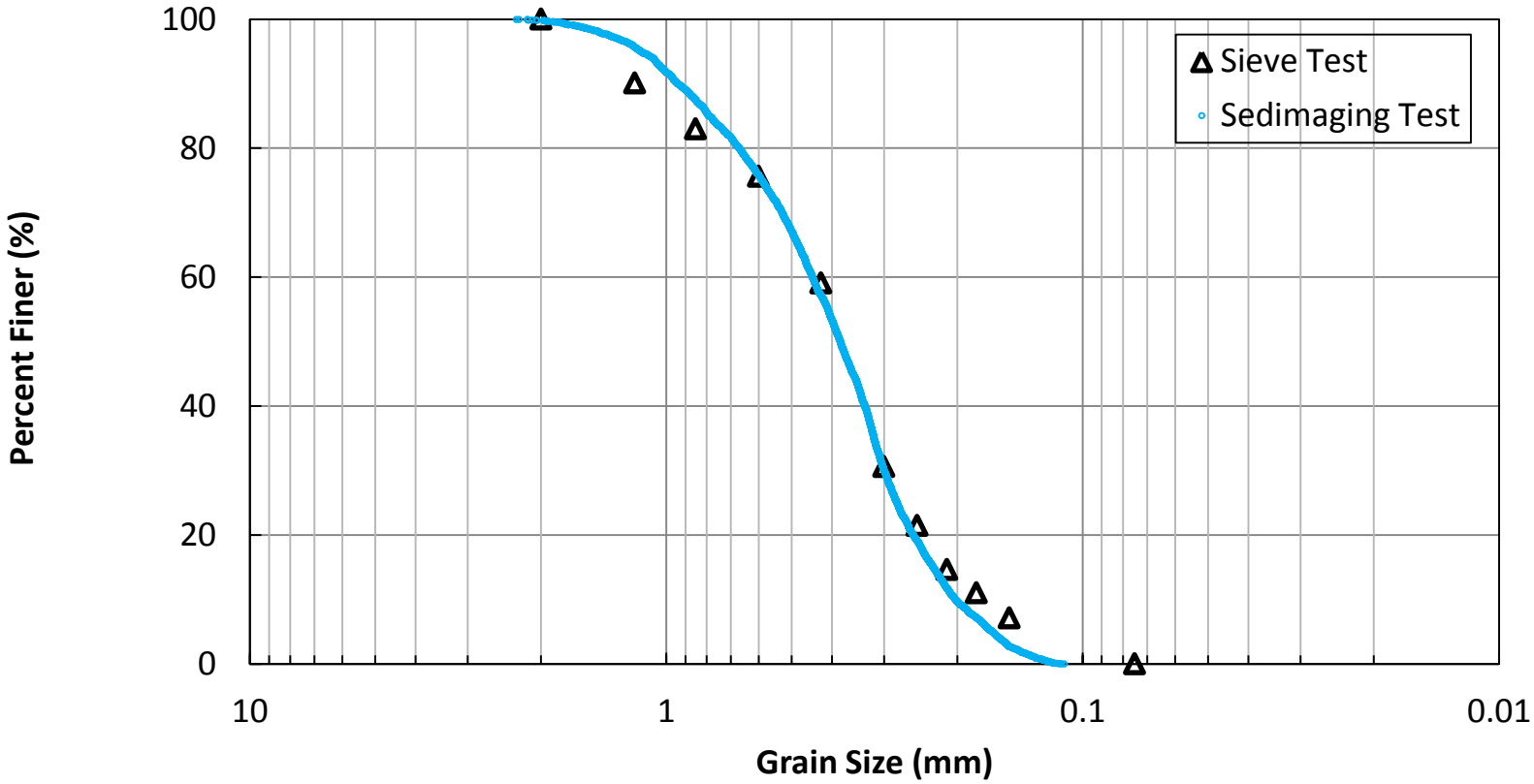

MATERIAL: Griffin w/o Fines

PIT NUMBER:

PIT NAME:

DATE SAMPLED: 04/22/11

SAMPLED BY: HS

DATE TESTED: 04/22/11

TESTED BY: HS

D_{60} (mm): 0.67

D_{30} (mm): 0.45

D_{10} (mm): 0.34

C_u: 1.94

C_g: 0.88

MAGNIFICATION (pix/mm): 33.6

IMAGE SIZE (pix): 4152 x 1280

IMAGE SIZE (mm): 123.6 x 38.1

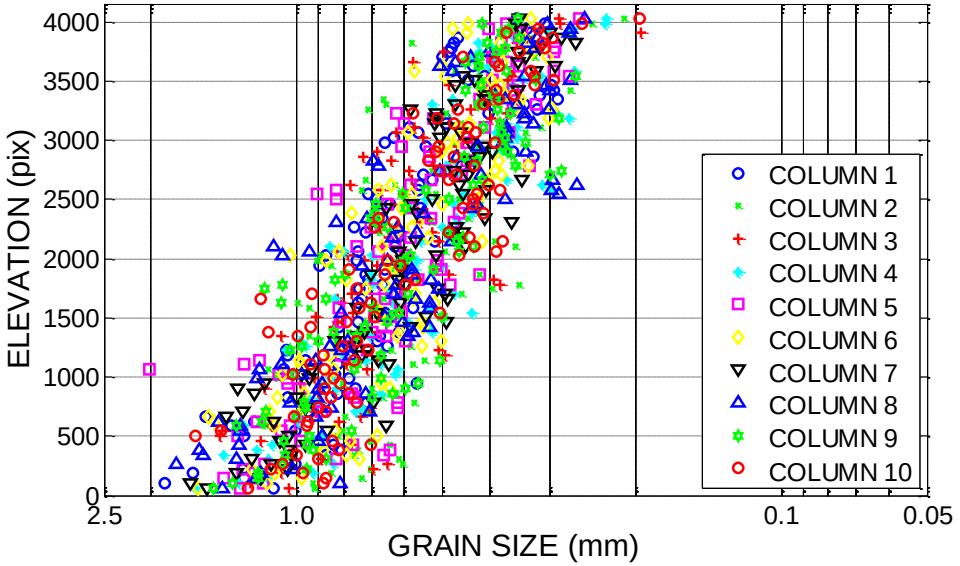

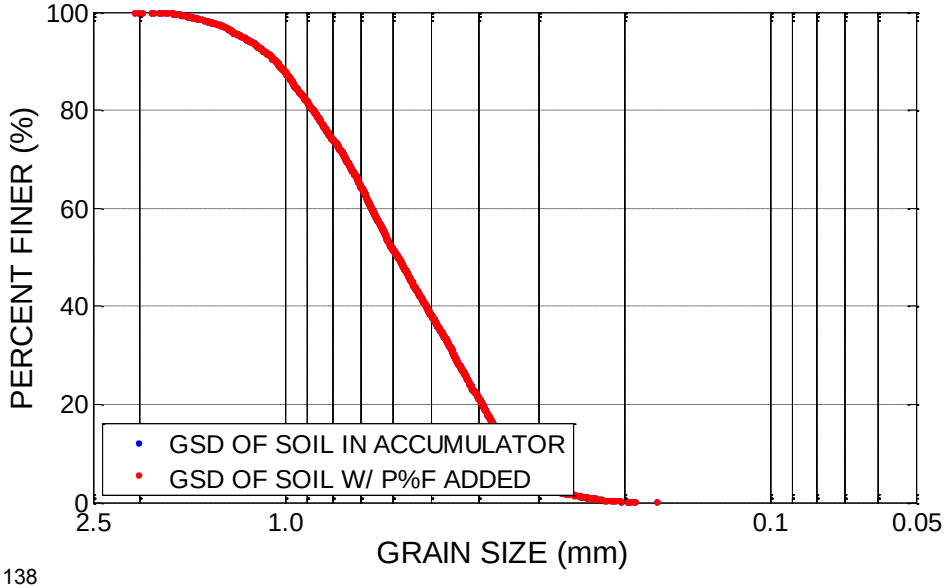

MATERIAL	PIT NUMBER	PIT NAME
Griffin w/o Fines		

DATE SAMPLED	SAMPLED BY	DATE TESTED	TESTED BY
04/22/11	HS	04/22/11	HS

	FRACTIONAL % RETAINED	CUMULATIVE % RETAINED	RESULTS % PASSING
NO. 10	0	0	100
NO. 20	22.1000	22.1000	77.9000
NO. 30	26.4000	48.5000	51.5000
NO. 40	25.8000	74.4000	25.6000
NO. 50	20.6000	94.9000	5.1000
NO. 60	3.7000	98.6000	1.4000
NO. 70	1	99.6000	0.4000
NO. 80	0.3000	100	0
NO. 100	0	100	0
NO. 200	0	100	0

Material: Griffin w/o Fines

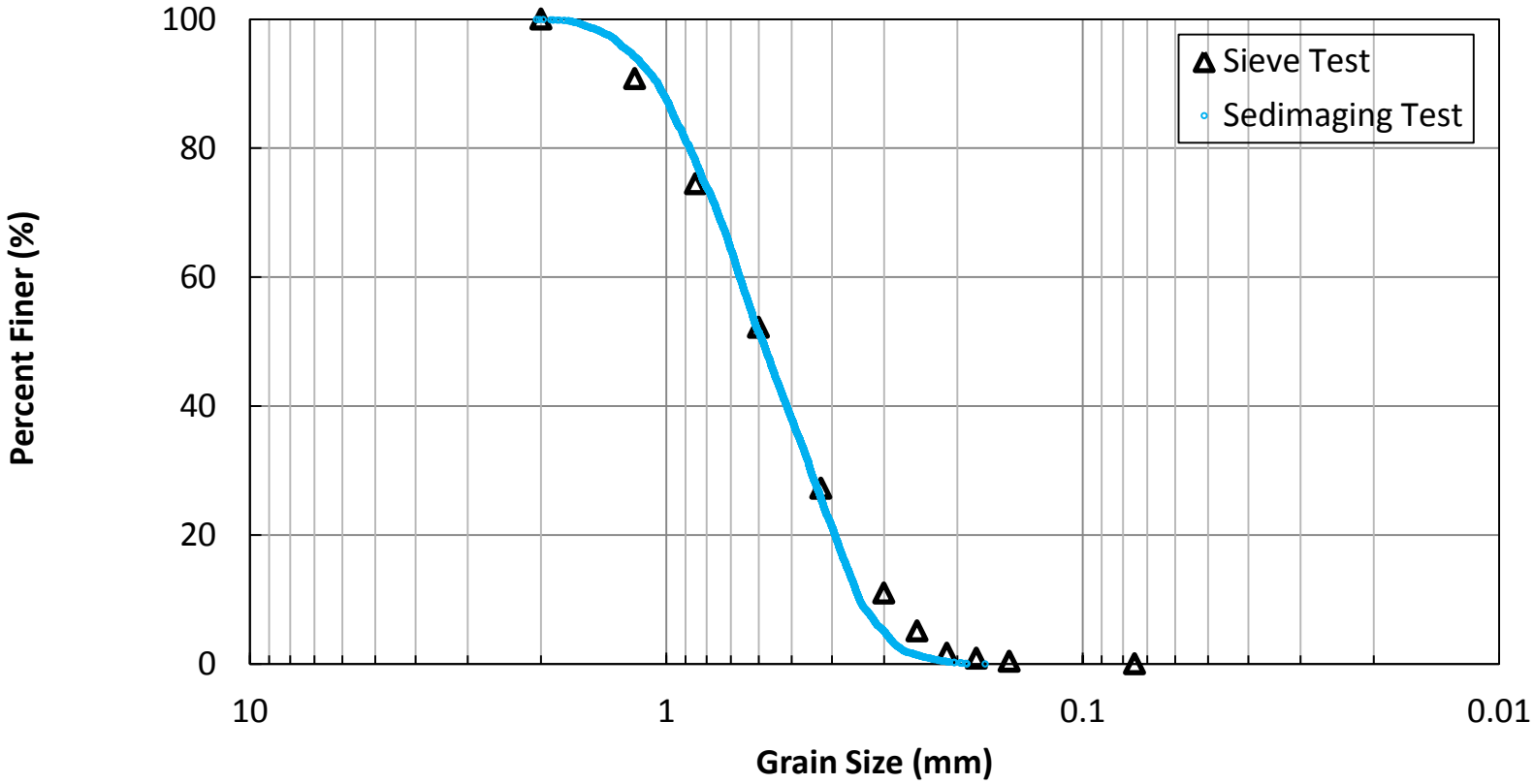

MATERIAL: 30A w/o Fines

PIT NUMBER:

PIT NAME:

DATE SAMPLED: 04/23/11

SAMPLED BY: HS

DATE TESTED: 04/23/11

TESTED BY: HS

D_{60} (mm): 0.53

D_{30} (mm): 0.27

D_{10} (mm): 0.15

C_u: 3.46

C_g: 0.89

MAGNIFICATION (pix/mm): 33.6

IMAGE SIZE (pix): 4136 x 1280

IMAGE SIZE (mm): 123.1 x 38.1

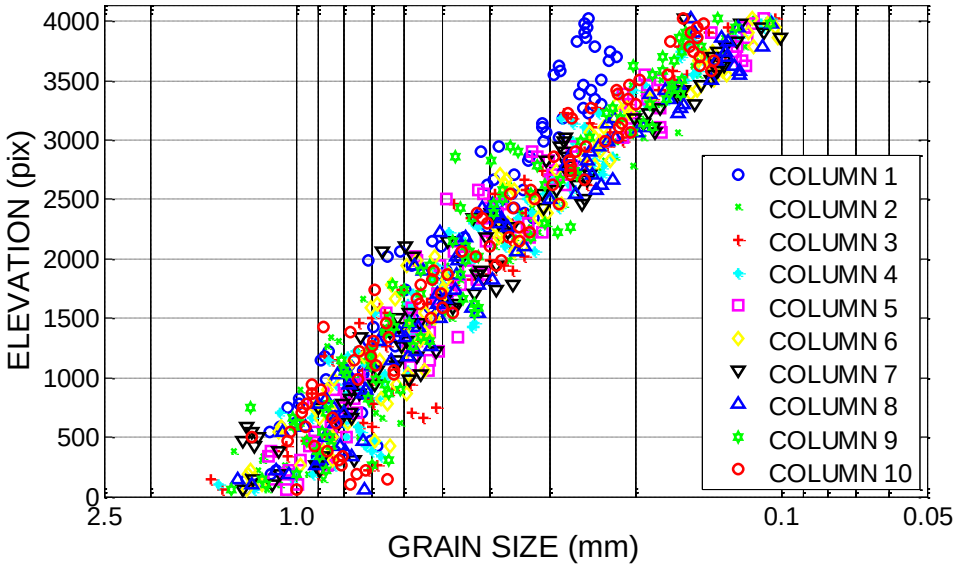

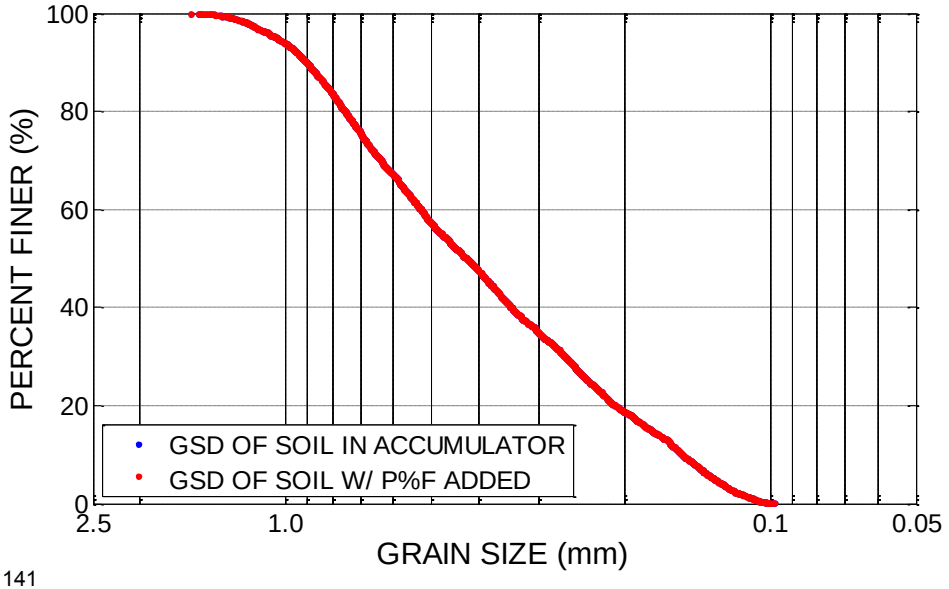

MATERIAL	PIT NUMBER	PIT NAME
30A w/o Fines		

DATE SAMPLED	SAMPLED BY	DATE TESTED	TESTED BY
04/23/11	HS	04/23/11	HS

	FRACTIONAL % RETAINED	CUMULATIVE % RETAINED	RESULTS % PASSING
NO. 10	0	0	100
NO. 20	13.1000	13.1000	86.9000
NO. 30	19.8000	32.8000	67.2000
NO. 40	17	49.8000	50.2000
NO. 50	15.3000	65.1000	34.9000
NO. 60	7.7000	72.8000	27.2000
NO. 70	6.8000	79.6000	20.4000
NO. 80	4.8000	84.4000	15.6000
NO. 100	6.1000	90.5000	9.5000
NO. 200	9.5000	100	0

Material: 30A w/o Fines*

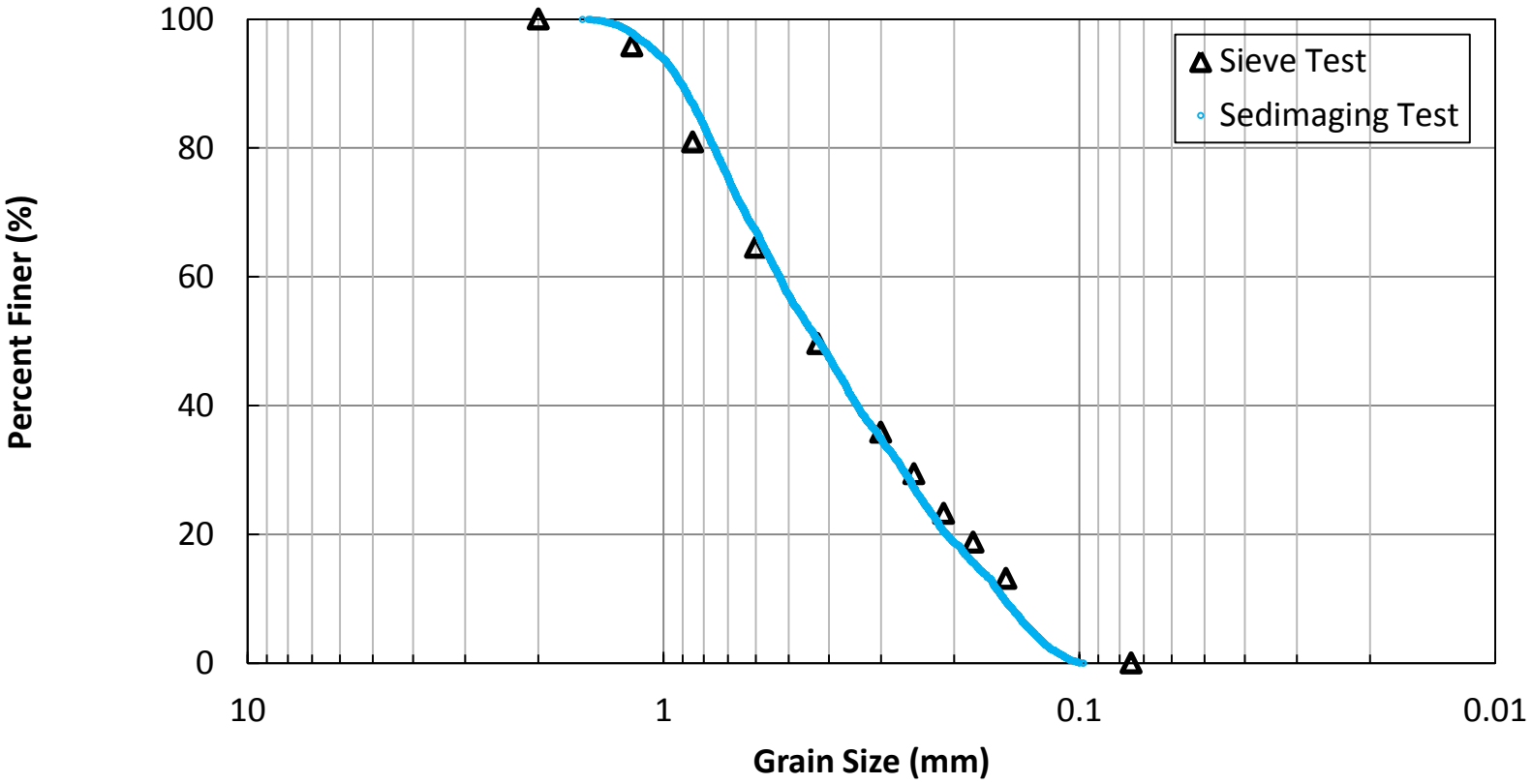

*** Specific calibration curve for 30A has been used.**

MATERIAL: Oakland County w/o Fines

PIT NUMBER:

PIT NAME:

DATE SAMPLED: 04/25/11

SAMPLED BY: HS

DATE TESTED: 04/25/11

TESTED BY: HS

D_{60} (mm): 0.37

D_{30} (mm): 0.24

D_{10} (mm): 0.19

C_u: 1.90

C_g: 0.84

MAGNIFICATION (pix/mm): 33.6

IMAGE SIZE (pix): 4072 x 1280

IMAGE SIZE (mm): 121.2 x 38.1

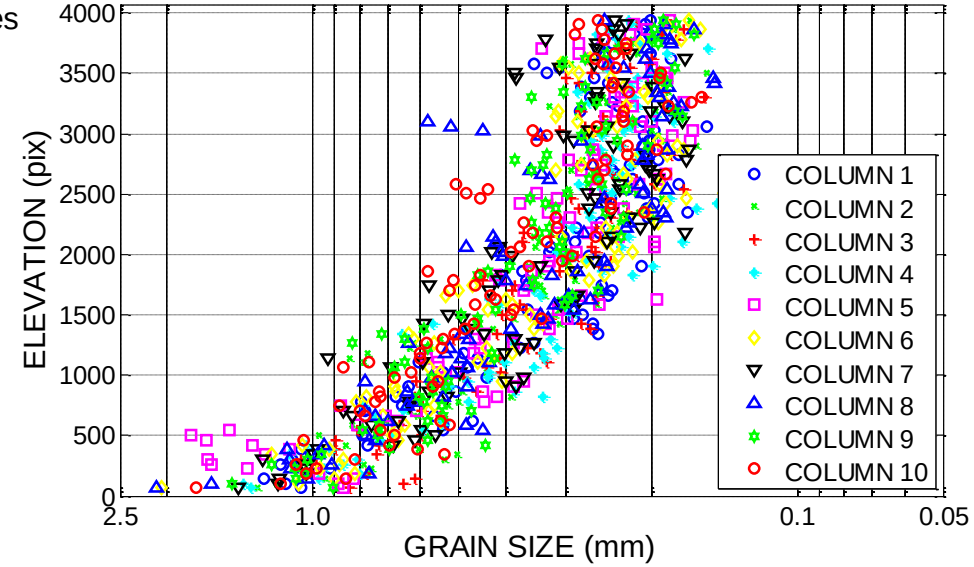

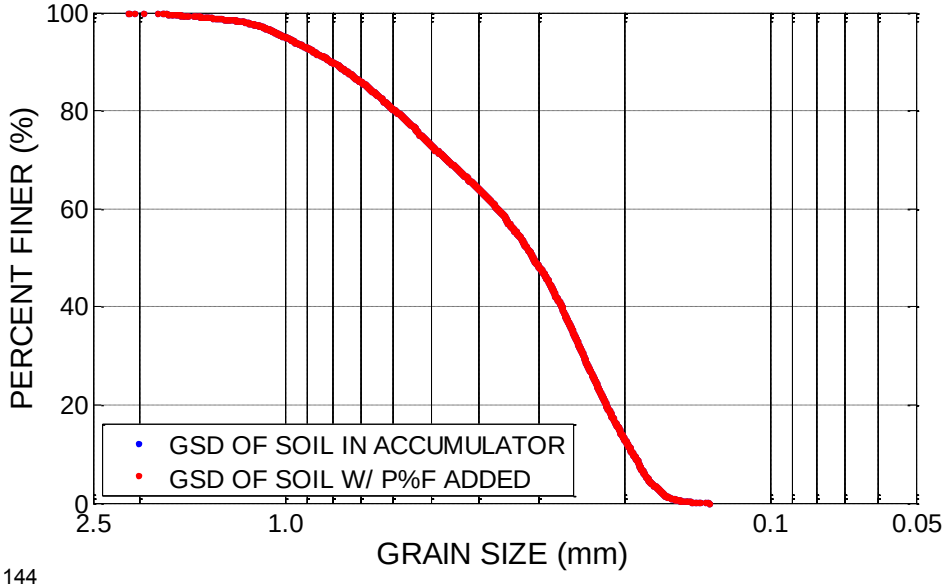

MATERIAL	PIT NUMBER	PIT NAME
Oakland County w/o Fines		

DATE SAMPLED	SAMPLED BY	DATE TESTED	TESTED BY
04/25/11	HS	04/25/11	HS

	FRACTIONAL % RETAINED	CUMULATIVE % RETAINED	RESULTS % PASSING
NO. 10	0.1000	0.1000	99.9000
NO. 20	8.5000	8.6000	91.4000
NO. 30	11.1000	19.7000	80.3000
NO. 40	13.7000	33.4000	66.6000
NO. 50	18.6000	51.9000	48.1000
NO. 60	15.3000	67.3000	32.7000
NO. 70	15.2000	82.5000	17.5000
NO. 80	12.3000	94.9000	5.1000
NO. 100	4.7000	99.6000	0.4000
NO. 200	0.4000	100	0

Material: Oakland County w/o Fines

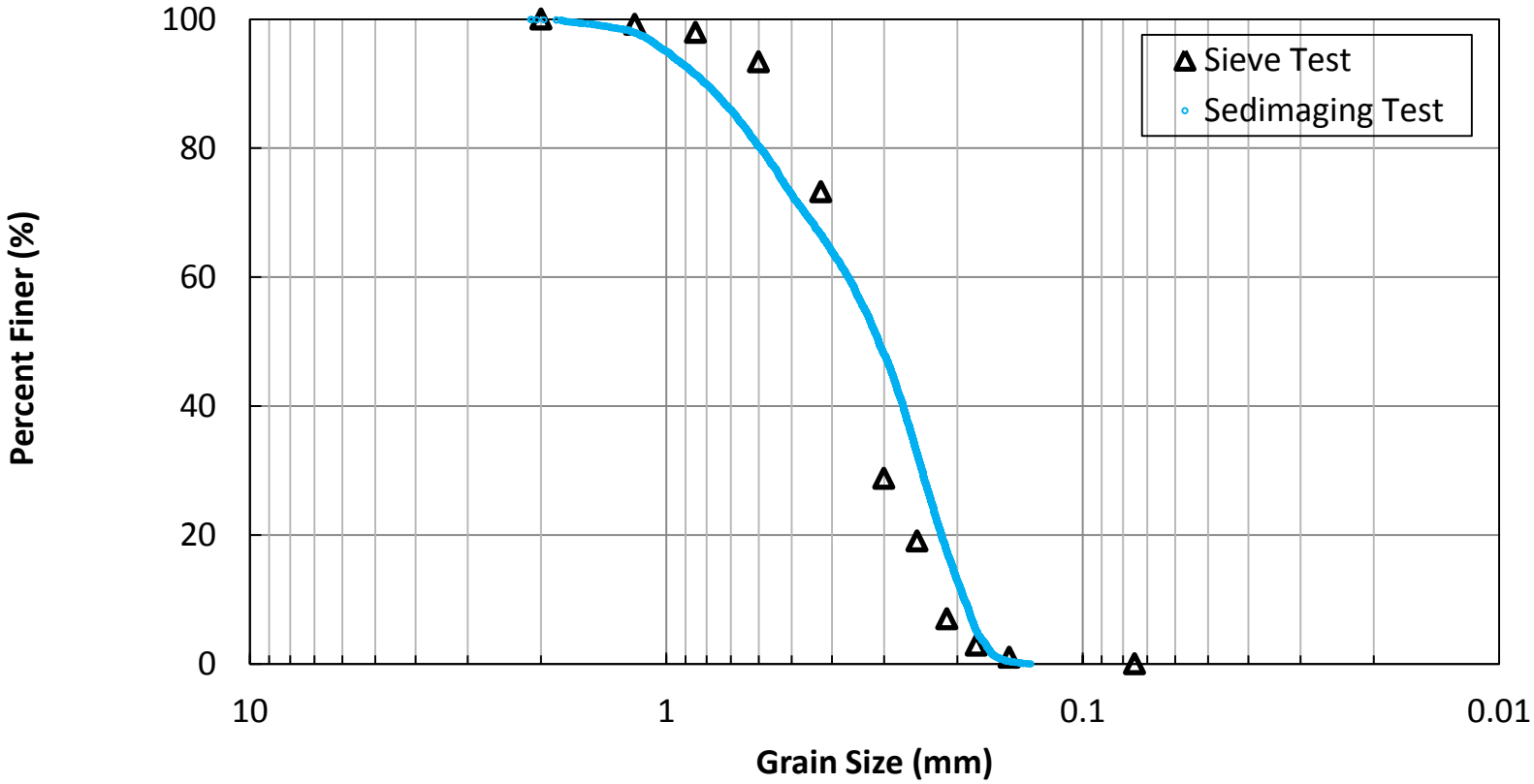

MATERIAL: Costa Rica w/o Fines

PIT NUMBER:

PIT NAME:

DATE SAMPLED: 04/30/11

SAMPLED BY: HS

DATE TESTED: 04/30/11

TESTED BY: HS

D_{60} (mm): 0.16

D_{30} (mm): 0.12

D_{10} (mm): 0.11

C_u: 1.49

C_g: 0.91

MAGNIFICATION (pix/mm): 33.3

IMAGE SIZE (pix): 4136 x 1280

IMAGE SIZE (mm): 124.2 x 38.4

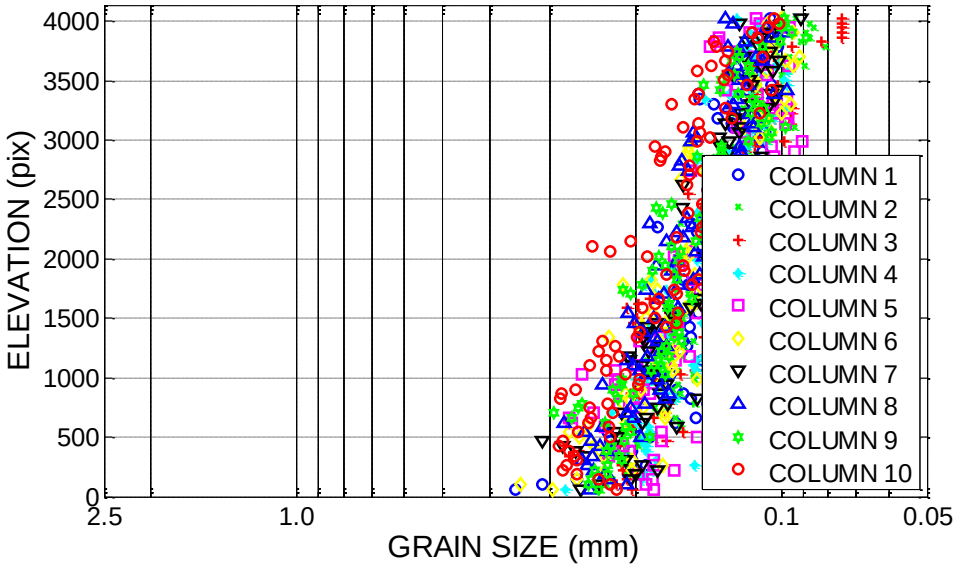

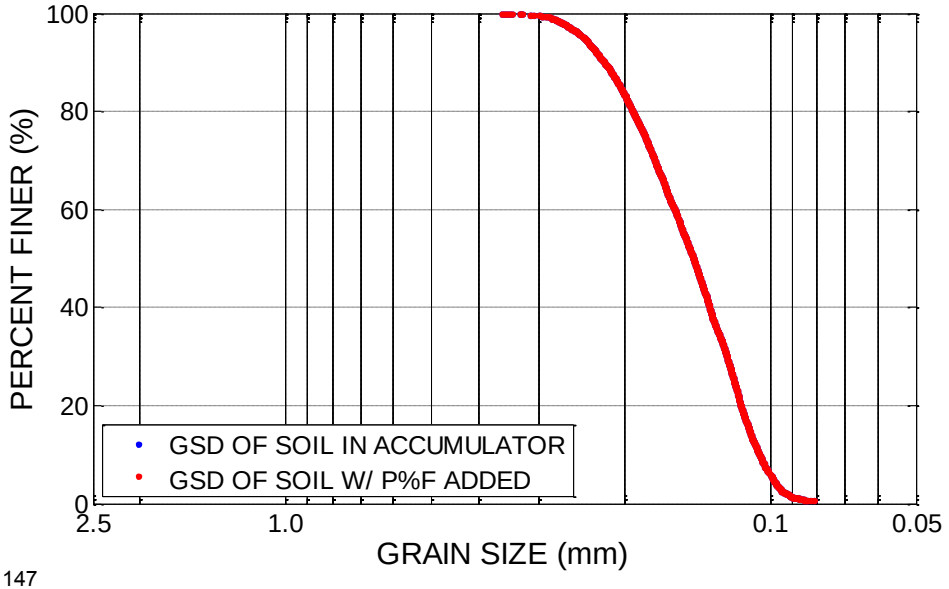

MATERIAL	PIT NUMBER	PIT NAME
Costa Rica w/o Fines		

DATE SAMPLED	SAMPLED BY	DATE TESTED	TESTED BY
04/30/11	HS	04/30/11	HS

	FRACTIONAL % RETAINED	CUMULATIVE % RETAINED	RESULTS % PASSING
NO. 10	0	0	100
NO. 20	0	0	100
NO. 30	0	0	100
NO. 40	0	0	100
NO. 50	0.4000	0.4000	99.6000
NO. 60	3.4000	3.8000	96.2000
NO. 70	8.3000	12.2000	87.8000
NO. 80	13.7000	25.9000	74.1000
NO. 100	19.6000	45.5000	54.5000
NO. 200	53.9000	99.4000	0.6000

Material: Costa Rica w/o Fines

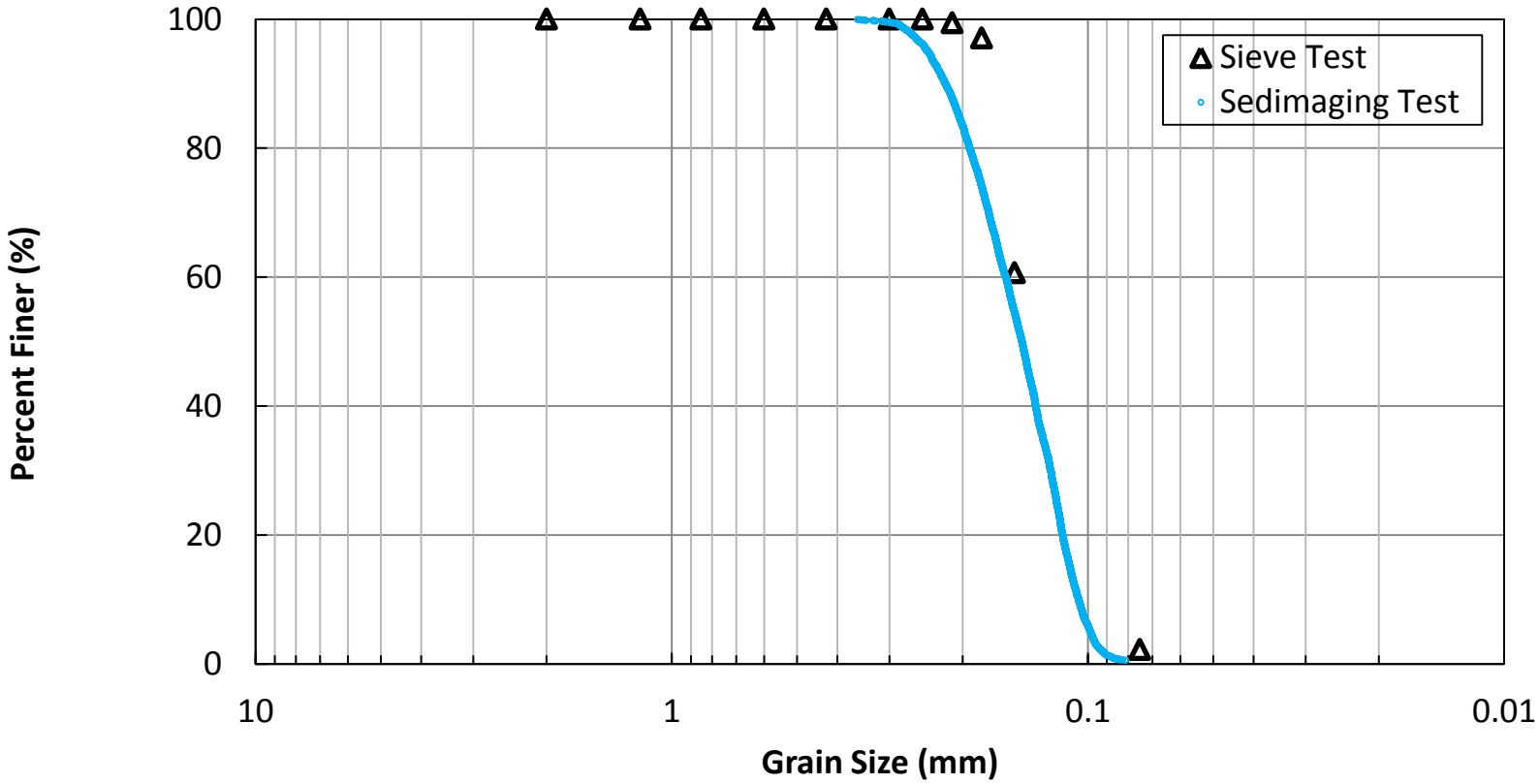

MATERIAL: Upper Peninsula w/o Fines

PIT NUMBER:

PIT NAME:

DATE SAMPLED: 05/05/11

SAMPLED BY: HS

DATE TESTED: 05/05/11

TESTED BY: HS

D_{60} (mm): 0.58

D_{30} (mm): 0.31

D_{10} (mm): 0.20

C_u: 2.88

C_g: 0.85

MAGNIFICATION (pix/mm): 33.5

IMAGE SIZE (pix): 3368 x 1280

IMAGE SIZE (mm): 100.5 x 38.2

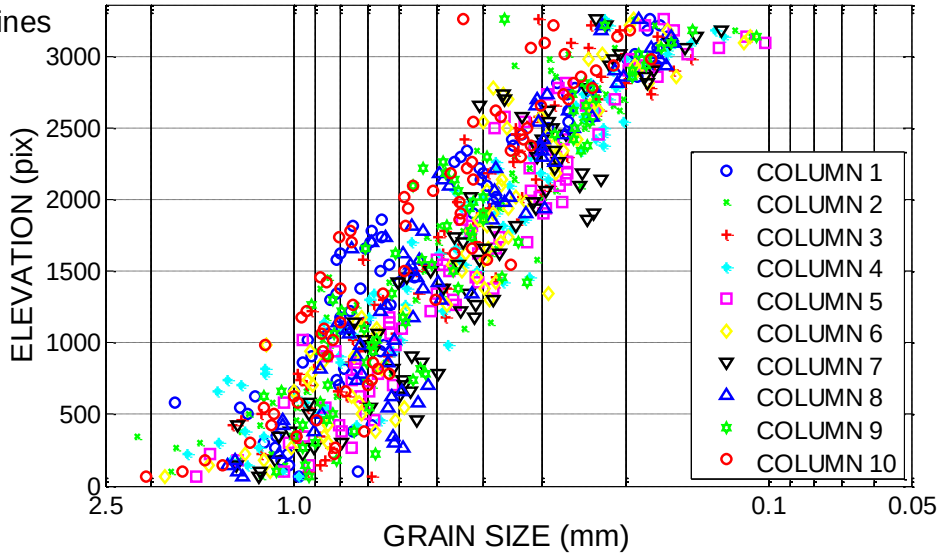

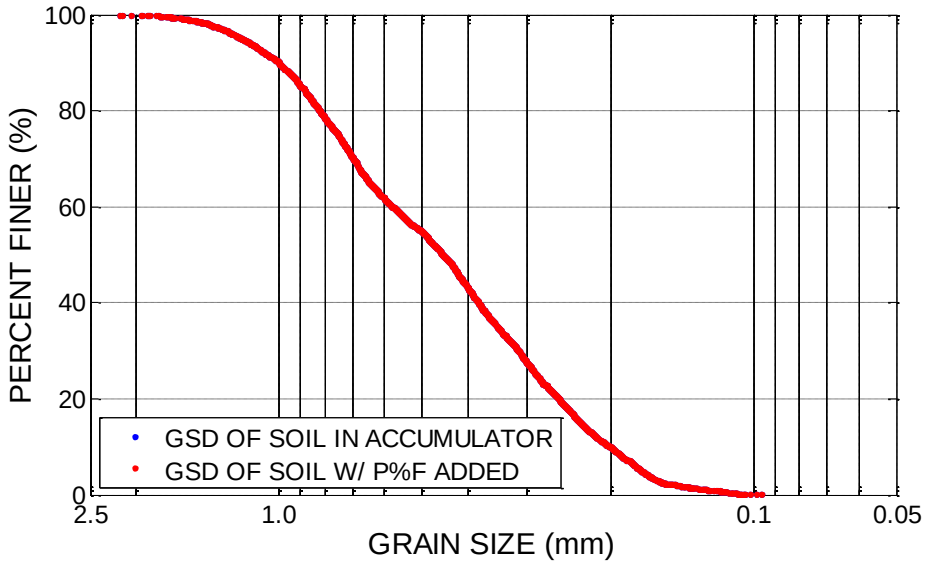

MATERIAL	PIT NUMBER	PIT NAME
Upper Peninsula w/o Fines		

DATE SAMPLED	SAMPLED BY	DATE TESTED	TESTED BY
05/05/11	HS	05/05/11	HS

	FRACTIONAL % RETAINED	CUMULATIVE % RETAINED	RESULTS % PASSING
NO. 10	0.1000	0.1000	99.9000
NO. 20	17.9000	18	82
NO. 30	20.3000	38.3000	61.7000
NO. 40	14.8000	53.1000	46.9000
NO. 50	19.4000	72.5000	27.5000
NO. 60	8.9000	81.4000	18.6000
NO. 70	7	88.4000	11.6000
NO. 80	5	93.4000	6.6000
NO. 100	4.4000	97.8000	2.2000
NO. 200	2.2000	100	0

Material: Upper Peninsula w/o Fines

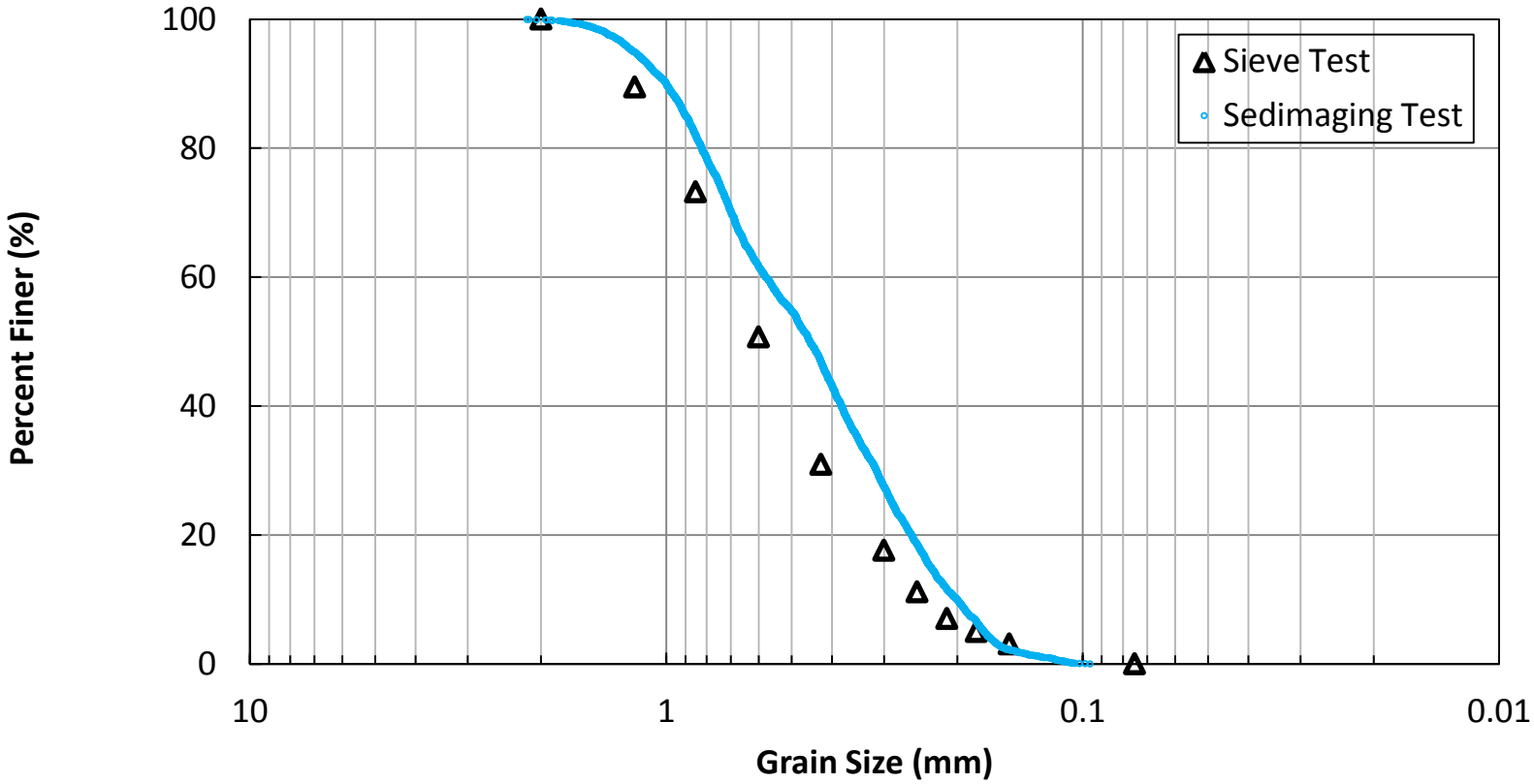

MATERIAL: 2NS w/ Fines Added

PIT NUMBER:

PIT NAME:

DATE SAMPLED: 05/08/11

SAMPLED BY: HS

DATE TESTED: 05/08/11

TESTED BY: HS

D_{60} (mm): 0.33

D_{30} (mm): 0.14

D_{10} (mm): 0.00

C_u: 0.00

C_g: 0.00

MAGNIFICATION (pix/mm): 33.4

IMAGE SIZE (pix): 4208 x 1280

IMAGE SIZE (mm): 126.0 x 38.3

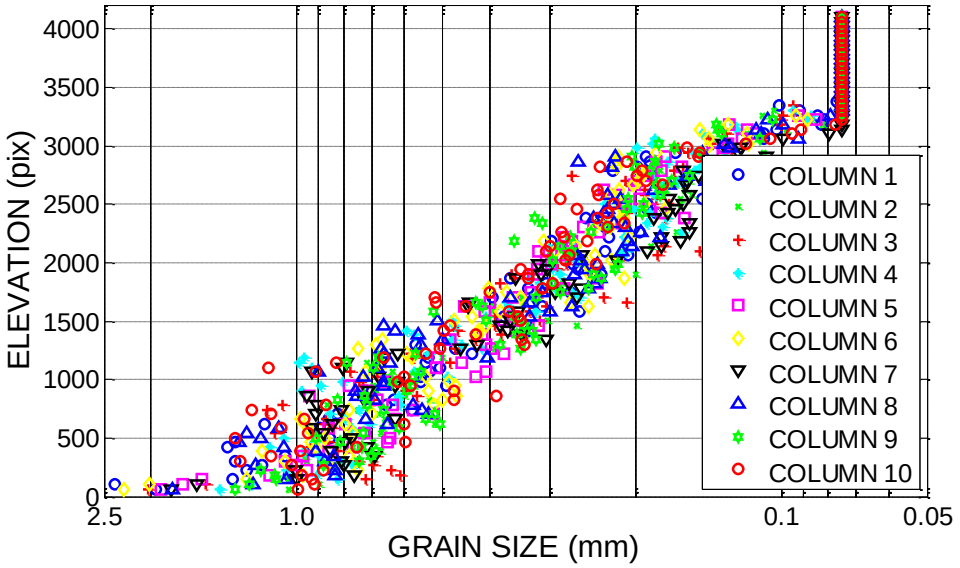

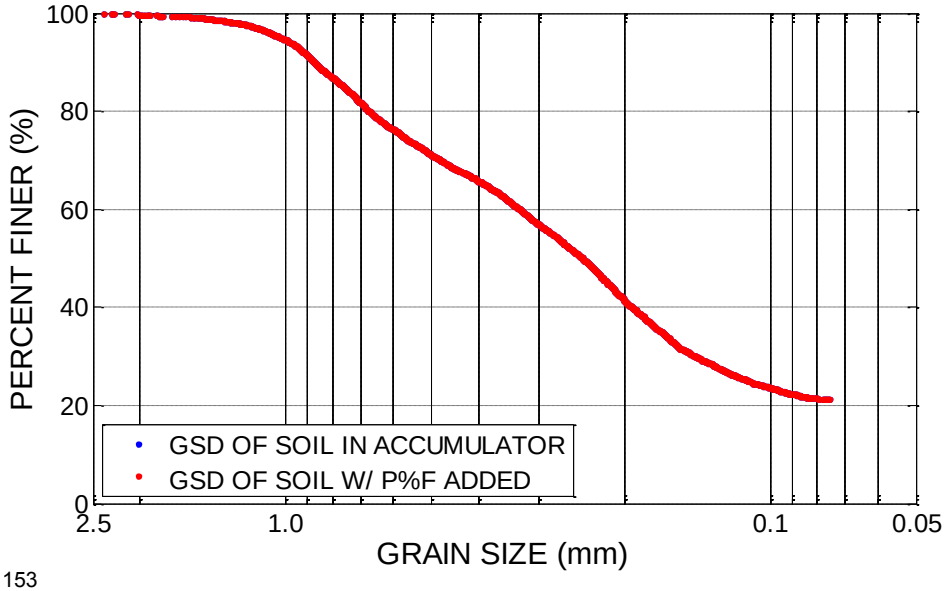

MATERIAL	PIT NUMBER	PIT NAME
2NS w/ Fines Added		

DATE SAMPLED	SAMPLED BY	DATE TESTED	TESTED BY
05/08/11	HS	05/08/11	HS

	FRACTIONAL % RETAINED	CUMULATIVE % RETAINED	RESULTS % PASSING
NO. 10	0.3000	0.3000	99.7000
NO. 20	10.8000	11.1000	88.9000
NO. 30	12.5000	23.6000	76.4000
NO. 40	9.1000	32.8000	67.2000
NO. 50	10.3000	43	57
NO. 60	6.1000	49.1000	50.9000
NO. 70	6.8000	55.9000	44.1000
NO. 80	6.7000	62.6000	37.4000
NO. 100	6.1000	68.7000	31.3000
NO. 200	10.1000	78.8000	21.2000

Material: 2NS w/ Fines Added

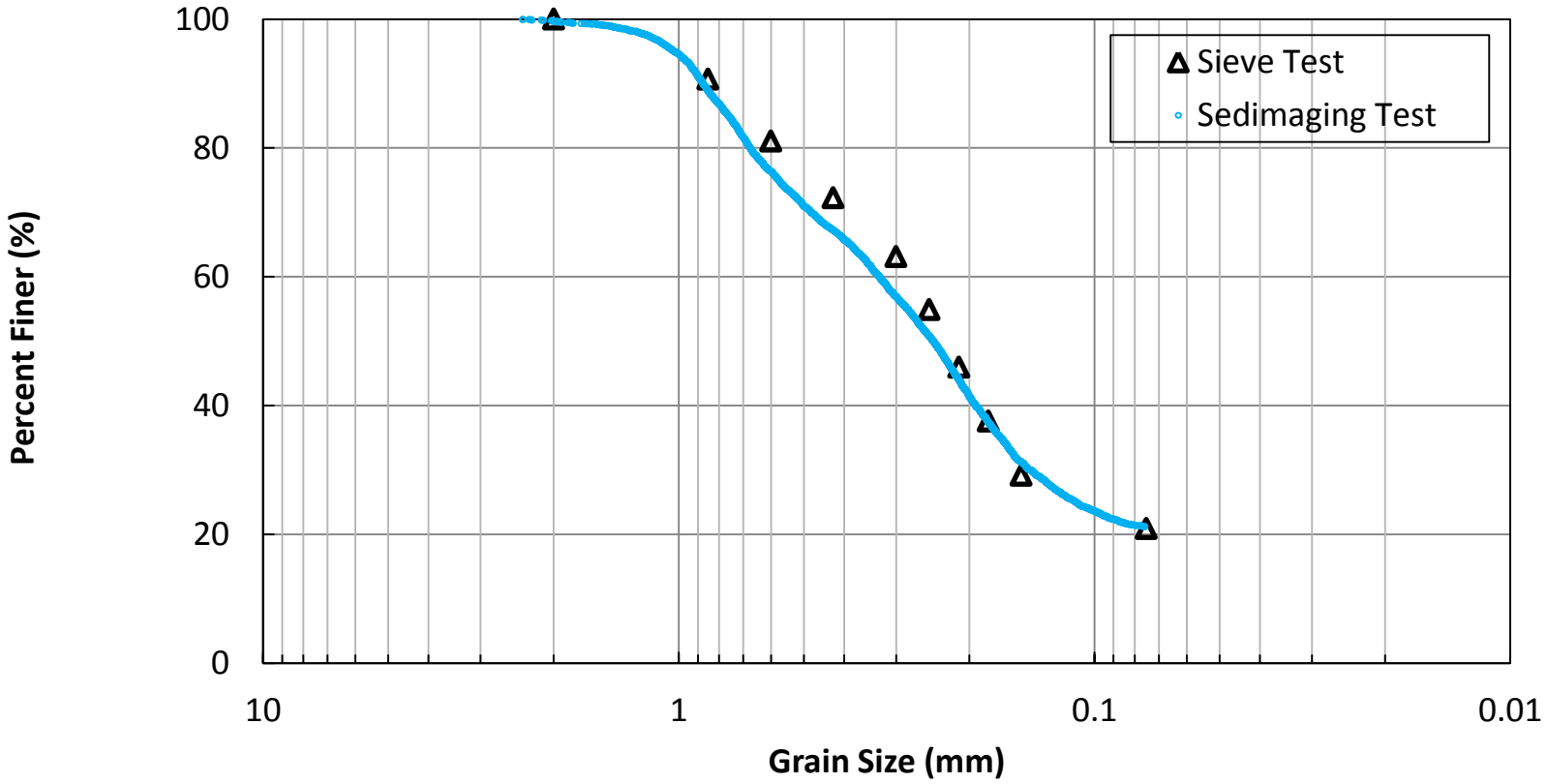

MATERIAL: Gabbro w/o Fines

PIT NUMBER:

PIT NAME:

DATE SAMPLED: 05/26/11

SAMPLED BY: HS

DATE TESTED: 05/26/11

TESTED BY: HS

D_{60} (mm): 0.77

D_{30} (mm): 0.46

D_{10} (mm): 0.26

C_u: 2.98

C_g: 1.06

MAGNIFICATION (pix/mm): 37.7

IMAGE SIZE (pix): 4552 x 1280

IMAGE SIZE (mm): 120.7 x 34.0

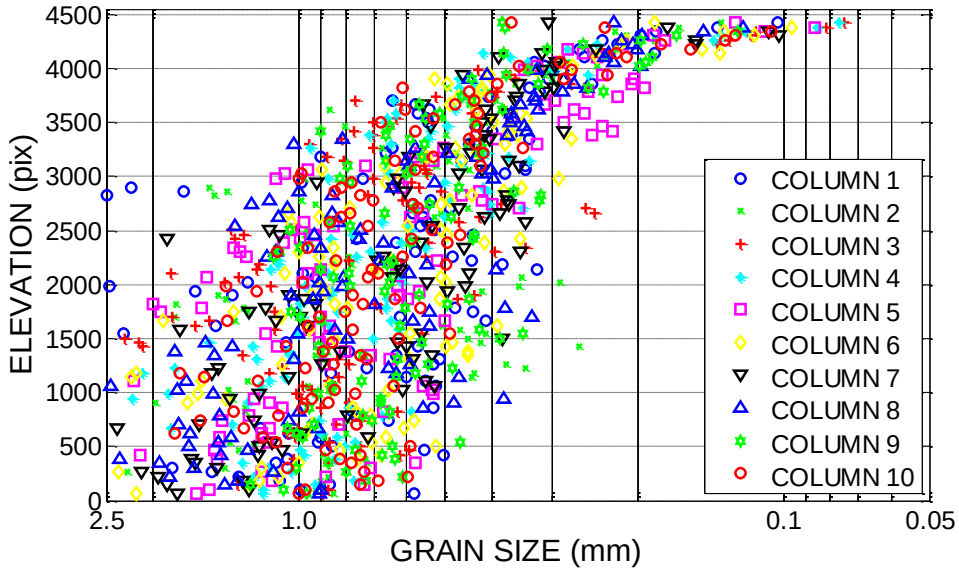

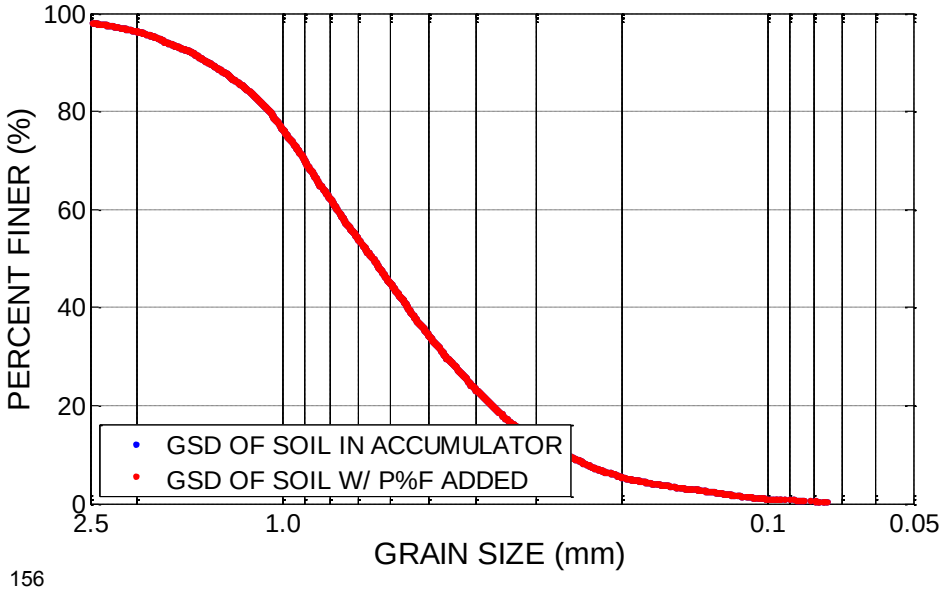

MATERIAL	PIT NUMBER	PIT NAME
Gabbro w/o Fines		

DATE SAMPLED	SAMPLED BY	DATE TESTED	TESTED BY
05/26/11	HS	05/26/11	HS

	FRACTIONAL % RETAINED	CUMULATIVE % RETAINED	RESULTS % PASSING
NO. 10	3.6000	3.6000	96.4000
NO. 20	30.7000	34.3000	65.7000
NO. 30	20.8000	55.1000	44.9000
NO. 40	18.7000	73.8000	26.2000
NO. 50	13.1000	86.8000	13.2000
NO. 60	4	90.8000	9.2000
NO. 70	2.9000	93.7000	6.3000
NO. 80	1.8000	95.5000	4.5000
NO. 100	1.3000	96.8000	3.2000
NO. 200	2.8000	99.6000	0.4000

Material: Gabbro w/o Fines*

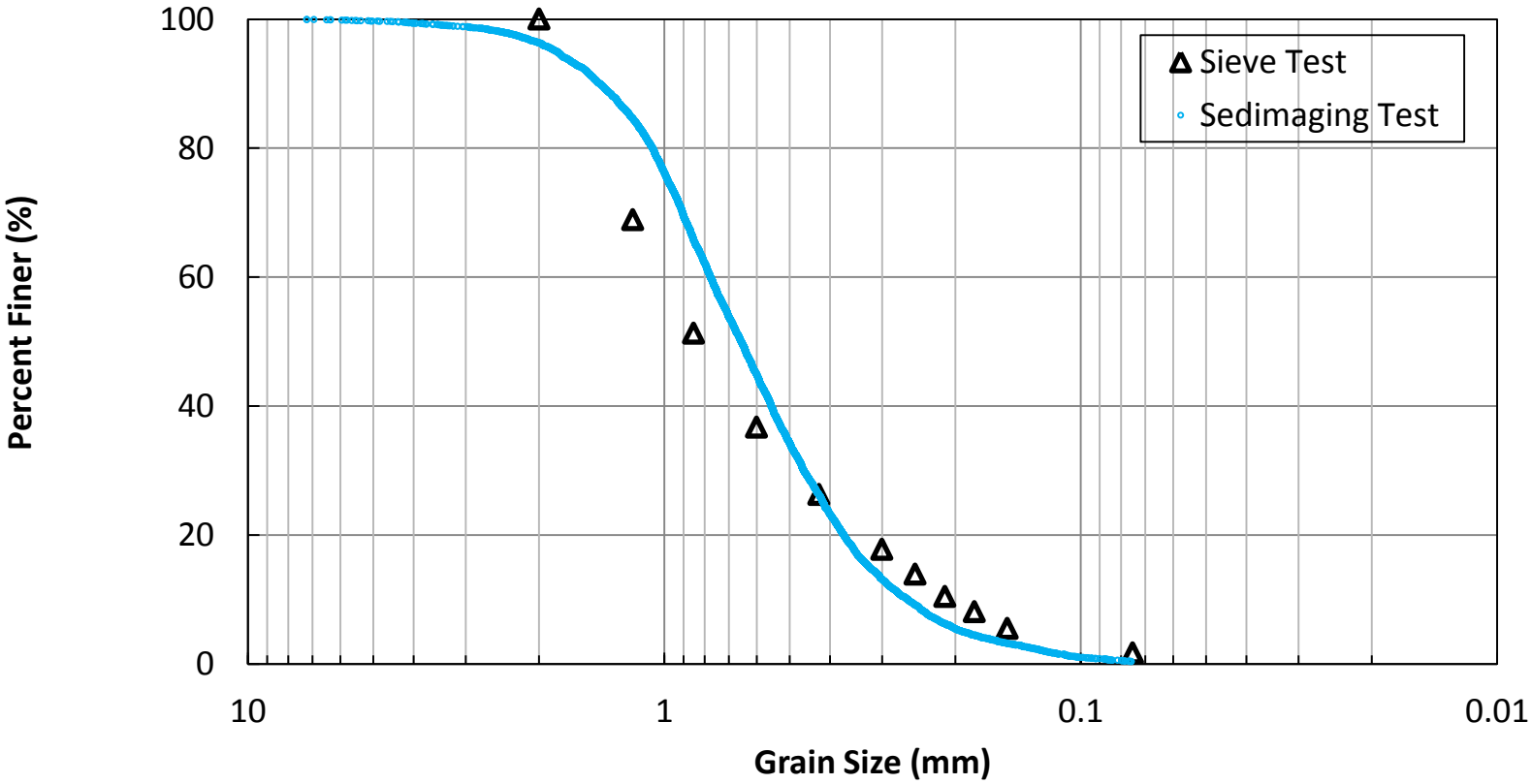

***Specific calibration curve for Gabbro has been used.**

MATERIAL: Class IIA w/ Fines

PIT NUMBER:

PIT NAME:

DATE SAMPLED: 08/26/11

SAMPLED BY: HS

DATE TESTED: 08/26/11

TESTED BY: HS

D_{60} (mm): 0.22

D_{30} (mm): 0.15

D_{10} (mm): 0.11

C_u: 2.04

C_g: 0.94

MAGNIFICATION (pix/mm): 36.6

IMAGE SIZE (pix): 4184 x 1280

IMAGE SIZE (mm): 114.3 x 35.0

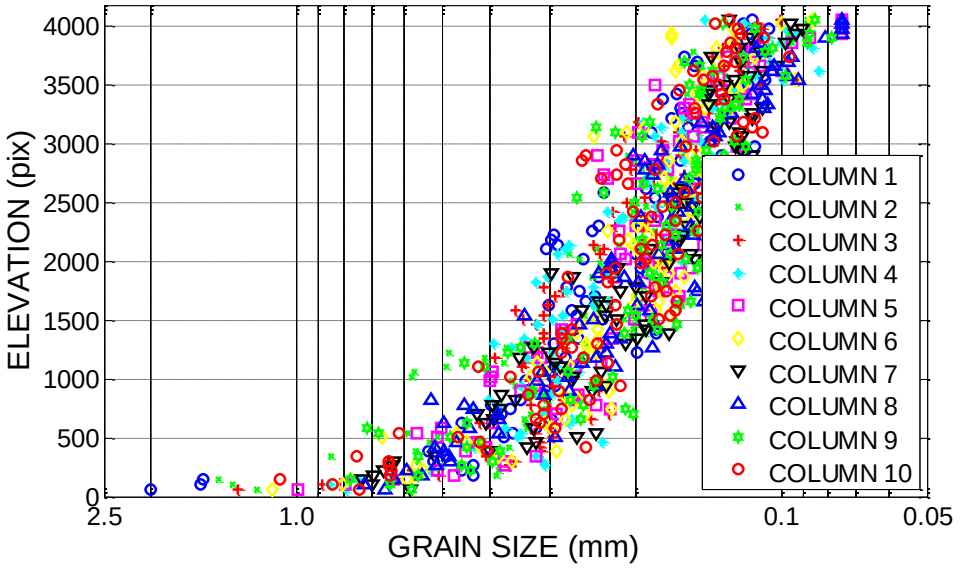

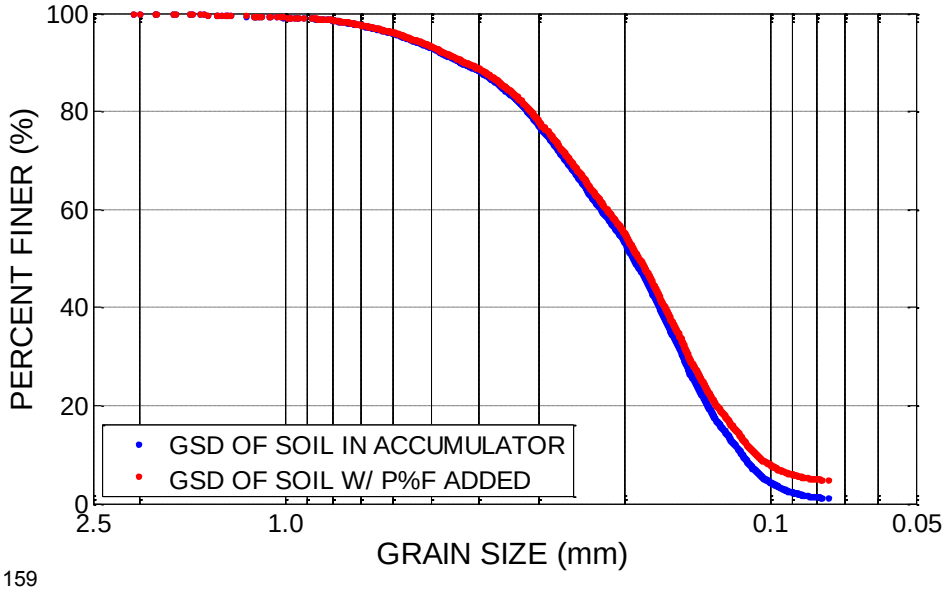

MATERIAL	PIT NUMBER	PIT NAME
Class IIA w/ Fines		

DATE SAMPLED	SAMPLED BY	DATE TESTED	TESTED BY
08/26/11	HS	08/26/11	HS

	FRACTIONAL % RETAINED	CUMULATIVE % RETAINED	RESULTS % PASSING
NO. 10	0.1000	0.1000	99.9000
NO. 20	1	1.1000	98.9000
NO. 30	2.7000	3.8000	96.2000
NO. 40	6.3000	10.1000	89.9000
NO. 50	12.1000	22.1000	77.9000
NO. 60	10	32.1000	67.9000
NO. 70	9.4000	41.5000	58.5000
NO. 80	11.3000	52.7000	47.3000
NO. 100	15.7000	68.5000	31.5000
NO. 200	26.7000	95.1000	4.9000

Material: Class IIA w/ Fines

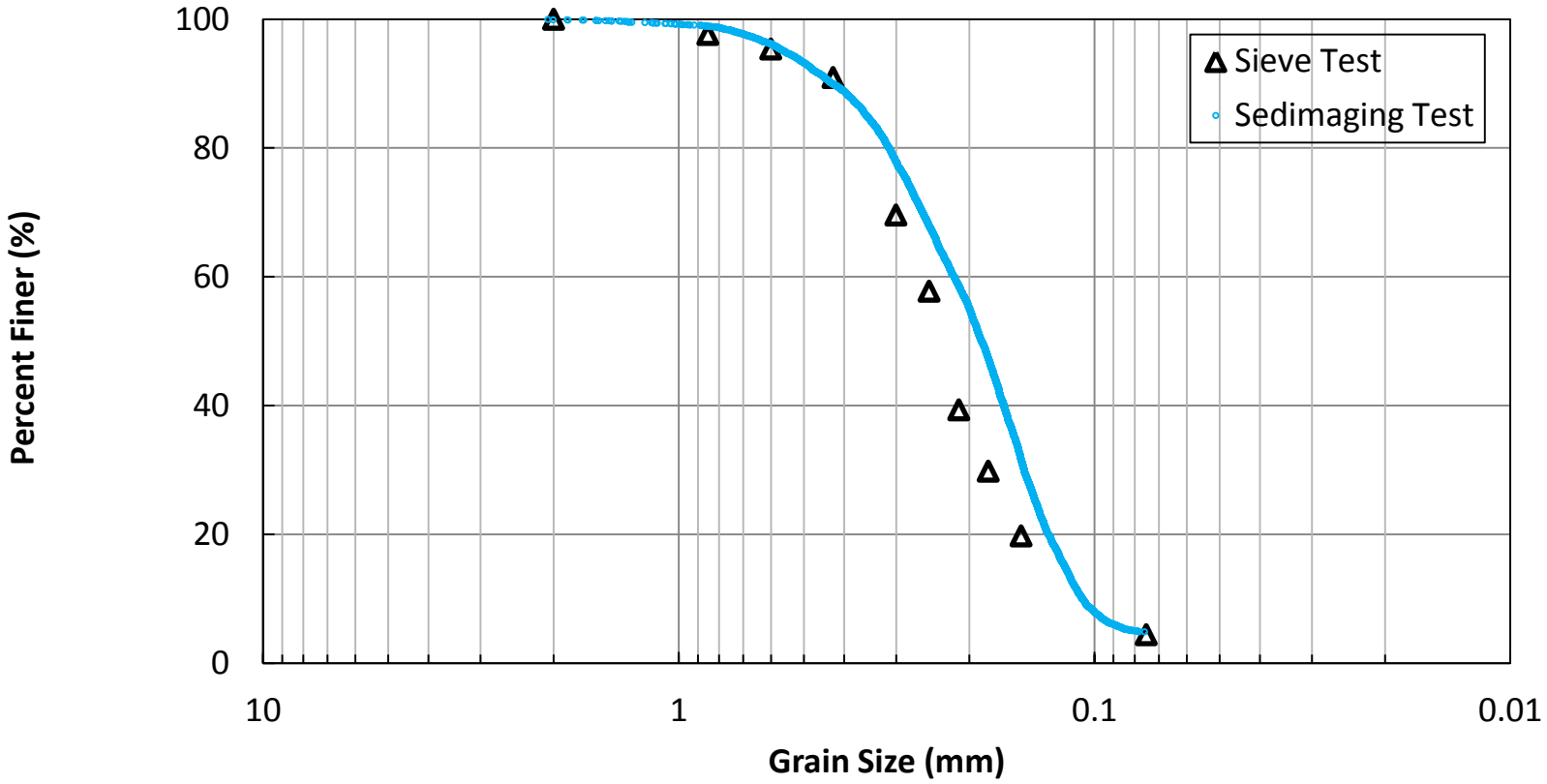

MATERIAL: Upper Peninsula w/ Fines

PIT NUMBER:

PIT NAME:

DATE SAMPLED: 08/30/11

SAMPLED BY: HS

DATE TESTED: 08/30/11

TESTED BY: HS

D_{60} (mm): 0.32

D_{30} (mm): 0.20

D_{10} (mm): 0.00

C_u: 0.00

C_g: 0.00

MAGNIFICATION (pix/mm): 36.7

IMAGE SIZE (pix): 3832 x 1280

IMAGE SIZE (mm): 104.4 x 34.9

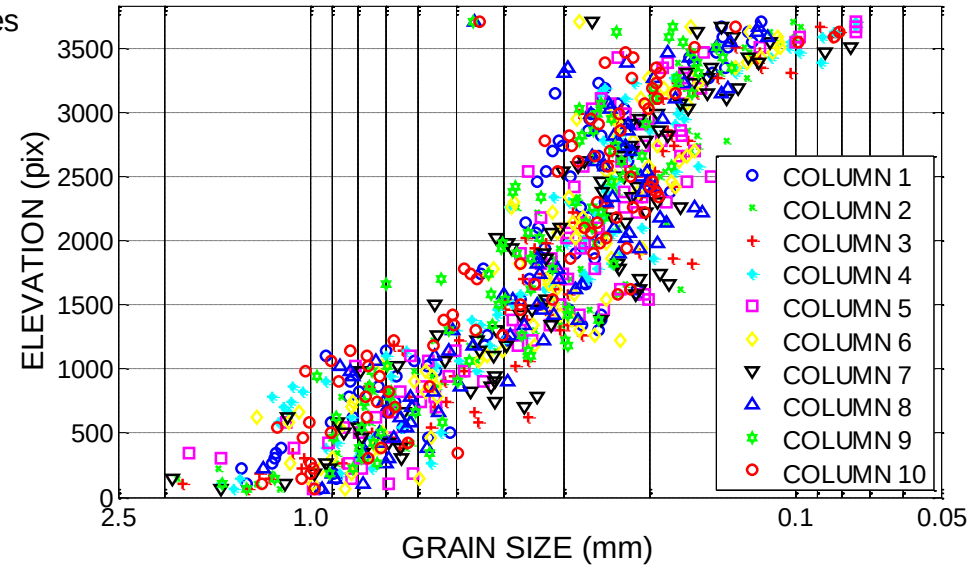

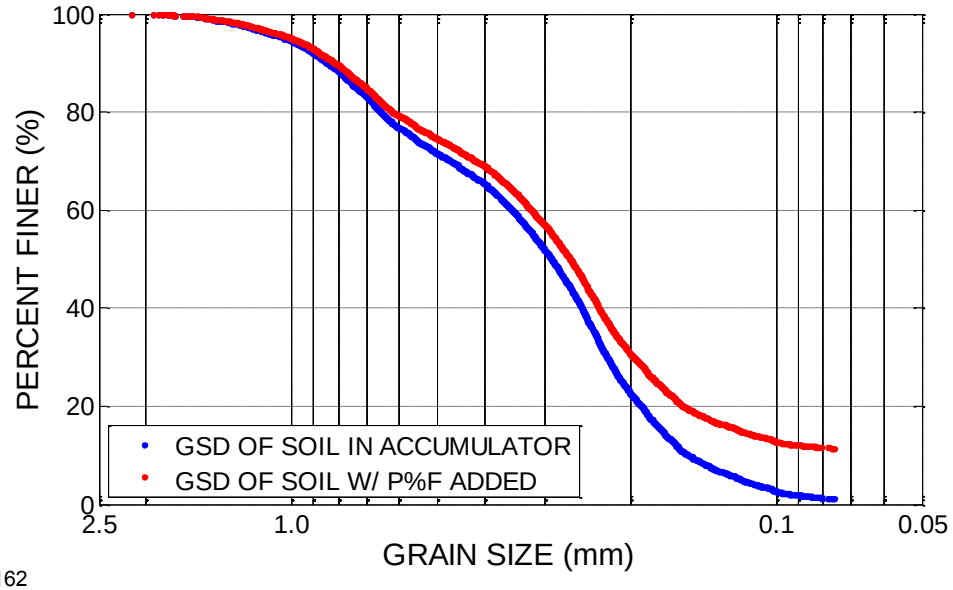

MATERIAL	PIT NUMBER	PIT NAME
Upper Peninsula w/ Fines		

DATE SAMPLED	SAMPLED BY	DATE TESTED	TESTED BY
08/30/11	HS	08/30/11	HS

	FRACTIONAL % RETAINED	CUMULATIVE % RETAINED	RESULTS % PASSING
NO. 10	0	0	100
NO. 20	8.8000	8.8000	91.2000
NO. 30	12	20.8000	79.2000
NO. 40	8.7000	29.4000	70.6000
NO. 50	13.7000	43.2000	56.8000
NO. 60	11.1000	54.3000	45.7000
NO. 70	11.8000	66.1000	33.9000
NO. 80	8.1000	74.2000	25.8000
NO. 100	6.6000	80.9000	19.1000
NO. 200	7.7000	88.6000	11.4000

Material: Upper Peninsula w/ Fines